Materials Advances

ROYAL SOCIETY OF CHEMISTRY

REVIEW

View Article Online
View Journal | View Issue

Check for updates

Cite this: *Mater. Adv.*, 2024, 5, 2622

Recent advances in cellulose nanocrystals-based sensors: a review

Shiva Singh,[a] Shakshi Bhardwaj,[a] Pragya Tiwari,[a] Keshav Dev,[b] Kaushik Ghosh[b] and Pradip K. Maji *[a]

Cellulose nanocrystals (CNCs) continue to pique the interest of researchers for sustainable development. These biopolymeric assemblies are significant because of their outstanding physical and chemical characteristics, inherent renewability, sustainability, and abundance. Given their large surface area, high aspect ratio, and abundant reactive surface groups, they are ideal for making probes for sensing applications. The present review highlights current advancements in developing CNCs-based sensors for sensing hazardous gases, metals, and solvents. It also discusses how CNCs-based sensors have evolved over the last decade. The review summarizes the methods mentioned in the literature for constructing and altering CNCs-based substrates using responsive compounds. Smart CNCs-based sensing probes for monitoring metals, chemicals, hazardous gases, humidity, and physical stimuli have received special attention. Several of the latest developments in smart sensors have also been evaluated and described. The review also includes the history of CNCs-based sensors, their evolution in the last decade, the challenges faced in their fabrication, and the future prospects of such sensing probes.

Received 25th August 2023,
Accepted 5th February 2024

DOI: 10.1039/d3ma00601h

rsc.li/materials-advances

[a] *Department of Polymer and Process Engineering, Indian Institute of Technology Roorkee, Saharanpur Campus, Saharanpur 247001, India. E-mail: pradip@pe.iitr.ac.in; Tel: +91-7895965010*
[b] *Department of Chemistry, Indian Institute of Technology, Roorkee 247667, India*

1. Introduction

The utilization of sensing technology across various domains has significantly enhanced the quality of human lifestyle in

Shiva Singh

Shiva Singh received his BSc degree in Chemistry (2017) from the University of Delhi (Delhi, India) and his MSc degree in Chemistry (2019) from the Visvesvaraya National Institute of Technology (VNIT Nagpur, India). He joined the Department of Polymer and Process Engineering, Indian Institute of Technology, Roorkee, India, in 2020, where he is pursuing his PhD under the supervision of Prof. Pradip Kumar Maji and Prof. Kaushik Ghosh. He received the most prestigious Prime Minister Research Fellowship in India for pursuing his research. His research is focused on the preparation of anti-counterfeiting and sensing materials from agro-waste-based liquid-crystalline nanocellulose composites. He has won many awards, including the Young Researcher Travel Award at the 38th International Conference of Polymer Processing Society, Switzerland, in 2023.

Shakshi Bhardwaj

Shakshi Bhardwaj obtained her BSc in Chemistry from the University of Delhi (Delhi, India) in 2017 and her MSc in Organic Chemistry from Maharshi Dayanand University (Rohtak, Haryana, India) in 2019. In 2022, she began her PhD studies in the Department of Polymer and Process Engineering, Indian Institute of Technology, Roorkee, India, under the direction of Prof. Pradip Kumar Maji. Her studies concentrated on hydrophobic cellulose nanofiber aerogels assisted by phase transition materials for thermal energy storage. She was awarded the most prestigious Prime Minister Research Fellowship in India for her research. She has received many awards for presenting her work at different conferences and seminars.

Open Access Article. Published on 08 Febwaliyo 2024. Downloaded on 12/09/2024 22:53:41.
This article is licensed under a Creative Commons Attribution-NonCommercial 3.0 Unported Licence.

© 2024 The Author(s). Published by the Royal Society of Chemistry

Open Access Article. Published on 08 Febwaliyo 2024. Downloaded on 12/09/2024 22:53:41.
This article is licensed under a Creative Commons Attribution-NonCommercial 3.0 Unported Licence.

numerous aspects. Sensors are devices that are capable of detecting and measuring changes in the surrounding environment.[1] They function by collecting signals or data from the source and subsequently initiating a predetermined response or reaction. Various sources, such as light, temperature, motion, and pressure, can be utilized. In multiple domains such as healthcare, fitness, manufacturing, and everyday activities, a diverse array of applications are employed, making use of cutting-edge sensing technology.[2] A sensor refers to a technical apparatus, component, or subsystem that identifies certain phenomena or alterations in its surroundings and transmits these data in an identifiable manner by humans or machines. A sensor can transform a physical phenomenon into a quantifiable digital or optical signal, which can then be identified, interpreted, or subjected to additional processing.

Researchers have demonstrated various sensor prototypes showing excellent performance. Such sensors are prepared by printing, coating, or laminating functional materials like graphene, carbon nanotubes (CNTs), nanocellulose, polypyrrole (PPy), and metal nanowires.[3–9] Graphene oxide (GO) was dip-coated on yarn and reduced to make a wearable strain sensor. The prepared sensor can identify slight speech vibrations and forceful human motions like jogging, walking, and jumping.[5] Multifunctional CNF/CNT/MXene aerogels were made *via* facile bidirectional freezing, inspired by natural wood's hierarchical tracheid structure. They have demonstrated good mechanical

Pragya Tiwari

Pragya Tiwari completed her BTech (Hons.) in Textile Technology from Uttar Pradesh Textile Technology Institute (Kanpur, Uttar Pradesh, India) in 2022. Currently, she is enrolled in MTech in the Department of Polymer and Process Engineering, Indian Institute of Technology Roorkee (Roorkee, India) under the supervision of Prof. Pradeep Kumar Maji. Her studies concentrated on bio-based cellulose nanocrystal-reinforced polymer composites and antimicrobial, superhydrophobic, and conductive textile surfaces for defense applications.

Keshav Dev

Keshav Dev received his BSc Hons degree in Chemistry (2018) from the University of Delhi (Delhi, India) and his MSc degree in Chemistry (2021) from the Visvesvaraya National Institute of Technology (VNIT Nagpur, India). He joined the Department of Chemistry, Indian Institute of Technology, Roorkee, India, in 2023, where he is pursuing his PhD under the supervision of Prof. Kaushik Ghosh and Prof. Pradip Kumar Maji. His research is focused on the nanocellulose-based materials and their applications in metal sensing.

Kaushik Ghosh

Kaushik Ghosh is a Professor at the Indian Institute of Technology, Department of Chemistry in Roorkee, India. He received his PhD in Chemistry from the Indian Association for the Cultivation of Science (IACS), India, under the supervision of Prof. Animesh Chakravorty. He was a Post-Doctoral Researcher (2002–2005) at the Department of Chemistry and Biochemistry, University of California at Santa Cruz (USA) with Professor Pradip K. Mascharak and Professor Ted Holman. His research areas of interest include coordination chemistry, metal complexes and their interactions with DNA and proteins, metal ion sensing, inorganic biochemistry, catalysis, and organometallic chemistry. He was awarded the DST-SERC Fast Track Scheme for Young Scientists. He has published over 100 papers in refereed journals and conference proceedings.

Pradip K. Maji

Pradip Kumar Maji is an Associate Professor at the Indian Institute of Technology, Department of Polymer and Process Engineering in Roorkee, India. He earned his PhD in Polymer Science and Technology from the Indian Institute of Technology in Kharagpur, India. His research areas of interest include cellulose-based biopolymers, functional nanomaterials, anti-counterfeiting, superthermal insulation, supercapacitors, oil–water separation, and rubber technology. In 2022, he was awarded the JSPS Invitational Fellowship by the Japan Society for the Promotion of Science. He worked as a Scientist-C at the Defence Research and Development Organisation (3 Base Repair Depot, Indian Air Force, Chandigarh, India). He is a visiting scientist at Kyoto University in Kyoto, Japan. He has published over 100 papers in refereed journals, many book chapters and few indian patents.

Open Access Article. Published on 08 Febwaliyo 2024. Downloaded on 12/09/2024 22:53:41.
This article is licensed under a Creative Commons Attribution-NonCommercial 3.0 Unported Licence.

strength and electrical conductivity. The pressure sensors made of CNF/CNT/MXene aerogels show good sensing performance and can capture human biosignals.[10] Nanocellulose has established itself as a potent sensing material and can be used in various applications of sensing.

The majority of nanosized cellulose is composed of cellulose nanofibers (CNFs) and cellulose nanocrystals (CNCs). CNFs are alternatively referred to as nano-fibrillated cellulose (NFC).[11–15] CNCs are alternatively referred to as nanocrystalline cellulose (NCC) or cellulose nanowhiskers (CNW), which are commonly used terms for them.[16–20] Despite sharing the same chemical structure, CNCs and bulk cellulose exhibit distinct differences in their physical, chemical, and biological properties. In contrast to bulk cellulose, which exhibits a combination of crystalline and amorphous regions, CNCs possess a significantly higher specific surface area, an elevated surface-to-volume ratio, enhanced tensile strength and modulus, and distinctive liquid-crystalline properties.

Through surface modification, these CNCs can be applied across various disciplines, including biology, electronics, photonics and chemistry.[21–25] CNCs have been employed to enhance the mechanical and dispersibility characteristics of materials, owing to their outstanding tensile strength, water dispersibility, and hydrophilicity. They have been employed as highly efficient reinforcing additives for several polymers, including poly(lactic acid),[26–29] poly(butylene succinate),[30–32] and elastomers (like natural rubber).[33–36] CNCs show suitable stimuli responses; they can behave as sensors and hence can be utilized in the sensing field. Typically, sensors are devices that convert a variety of chemical, environmental, physical, and biological stimuli into analyzable output. They are classified as chemical, gas, ion, strain, and biological sensors according to their specificity for various analytes.[37–41] Diverse sensing methods have limitations, such as metal oxide degradation, posing a recyclability crisis. Similarly, a wide range of graphene-based sensors are not sensitive due to diminished exfoliation at elevated concentrations. However, nanocellulose (NC) could increase the sensing ability of graphene-based composites by inhibiting agglomeration.[42,43]

CNCs and conducting polymers have enhanced synergistic effects in glucose biosensing, water defluorination, strain sensing, flame resistance, supercapacitors, and cancer therapy.[44–47] In recent years, numerous nanocellulose-based composites have been developed; however, only a small number of review studies have summarised the sensing applications of CNCs-based composites. Some researchers have recently reviewed the applications of nanocellulose-based composites in various fields, including biosensing, aerogels, polymer composites, energy storage, *etc.*[48–51] There has been limited research describing the sensing applications of CNCs-based materials. In recent years, however, numerous summaries of biosensing applications have been published. Lv and colleagues summarized the nanocellulose-derived materials and their evolution in chiral photonics, flexible energy storage devices, and actuator applications.[52] Dai and co-workers summarised the 1D, 2D, and 3D forms of nanocellulose and their influence on sensing properties in 2020.[53] The literature still lacks a well-structured report on CNCs based sensors and their importance in gas, metal, chemical, biomaterial and physical stimuli sensing. In this review, we have presented a detailed discussion of how CNCs-based sensors are being utilized in sensing various stimuli, the history of CNCs-based sensors over the last decade, and the challenges involved in their preparation and applications.

2. Overview of cellulose and its nanodimensional characteristics

There is substantial scholarly interest in utilizing biobased polymers as substitutes for petroleum-derived alternatives within the industrial sectors. Prominent examples of biopolymers encompass chitosan, collagen, cellulose, pectin, and starch.[54–56] Cellulose, the prevailing biopolymer, has an annual production rate of around 1.5×10^{12} tonnes and finds application in a wider range of products compared to any other sustainable polymer.[8,36,57–65] Recently, there has been growing interest in nano-cellulosic materials due to their versatile applications and unique properties.[7,36,66–68] Consequently, cellulose is a promising material for developing sensors that exhibit enhanced sensing sensitivity.[69] The cellulose structure is characterized by a polymer with a linear chain consisting of 1,4-glycosidic linkages between D-glucopyranose subunits. Each glucose unit in the cellulose chain possesses three hydroxyl (–OH) groups, with the exception of the terminal units that possess four hydroxyl groups.[70–72] –OH groups in cellulosic materials contribute to various characteristics, including biodegradability, chirality, hydrophilicity, and others. When cellulose undergoes size reduction, it exhibits additional distinctive characteristics.[73] It has been discovered that cellulose, a condensation polymer and a natural homopolysaccharide, is the most prevalent organic substance, as it is abundantly available, cheap, renewable, biodegradable, and non-toxic.[74] At the nano-level, cellulose can have unique properties, which can be utilised for high end applications.

2.1. Classification of cellulose at the nano-level and its versatile applications

Crystalline nanocellulose (CNC), cellulose nanofibers (CNFs), and bacterial nanocellulose (BNC) are the three typical forms of nanocellulose (NC). Despite the fact that each of these falls within the nanoscale range, variations in form, size, and composition are possible. CNC and CNFs are both nanocelluloses derived from plants, whereas BNC is a microbial-based nanocellulose.[8,75–78] Typically, the diameters of CNC, CNFs, and BNC fall within the following ranges: 3–70 nm, 2–20 nm, and 20–100 nm. In contrast, the length of CNCs is between 70 and 300 nanometers, whereas those of CNFs and BNC are in the micron range. Mechanical, physical, and chemical disintegration of plant cellulose, or a combination thereof, is required for the fabrication of CNFs and CNCs.[66,78–80] Biotechnology is the only method by which microorganisms can be

© 2024 The Author(s). Published by the Royal Society of Chemistry

Open Access Article. Published on 08 Febwaliyo 2024. Downloaded on 12/09/2024 22:53:41.
This article is licensed under a Creative Commons Attribution-NonCommercial 3.0 Unported Licence.

utilised to produce BNC; it possesses superior purity, mechanical stability, and an interconnecting micropore arrangement similar to CNCs and CNFs.[81–83] The Mobile Matrix Reservoir Technology (MMR Tech), which was recently developed, has proven to be highly advantageous for regulating the configuration, dimensions, surface characteristics, and nanonetwork architectures of BNC.[84]

NC with high surface area and aspect ratio, dispersion stability, outstanding mechanical properties, and abundant active functionalities (hydroxyl and sulphone) on its surface make it suitable to combine with conductive polymers to produce sustainable nanocomposites for sensing purposes. NC-based nanohybrids are used for metal sensing in biological samples, water quality monitoring, *etc.* Such nanocomposites exhibit a piezoelectric effect promoted by hydrogen bonding of NC.[85] NC incorporated with polyaniline finds application in sensing electrochemical and optical responses. NC-integrated films are exploited in anti-counterfeiting and security encryption.[86]

Apart from these, NC has potential applications in triboelectric nanogenerators (TENGs). NC demonstrates notable qualities such as skin compatibility, friendliness, degradability, and recyclability. These attributes render cellulose an appealing candidate for the sustainable advancement of TENGs, particularly in lieu of the conventional nondegradable triboelectric active layers that are vital for the electrical output performance of TENGs. In contrast, unadulterated cellulose exhibits neutral properties when compared to other triboelectric series materials that function as active triboelectric components. By loading substrates made of other materials with a small quantity of NC, an electron loss tendency can be introduced, contact area can be increased, and TENG performance can be enhanced. Peng *et al.* incorporated NC into PDMS at a concentration of 2.5% by weight and utilised spin coating to fabricate the NC/PDMS composite film. A contact-separation TENG device was fabricated, featuring a positive electrode composed of Al and a negative electrode composed of the NC/PDMS film. The active layer area of the device was 2.25 cm^2. When subjected to an external force condition of 40 N at 10 Hz, the NC/PDMS–Al TENG produced an open circuit voltage of 320 V and a short circuit current of 11.25 μA. These values were two and four times greater, respectively, than those of the plain PDMS–Al TENG that did not incorporate NC.[87] In another report, to prepare TOCN–SH containing sulfhydryl groups, Roy *et al.* modified TONC (TEMPO oxidised NC) with 3-mercaptopropyltrimethoxylsilane (MPTMS) and subsequently treated it with allicin (Alc). By means of a thiol–ene click reaction conducted at 80 °C, the terminal alkene groups of allicin can undergo a complete and gentle reaction with the SH groups of TOCN in order to produce an allicin-modified TOCN (Alc/TONC) film characterised by a coarser surface. Allicin's S═O bond can significantly increase the Alc/TONC film's electron-donating capability. By employing the modified film as the positive electrode and PVDF as the negative electrode, the author successfully constructed a contact-separation TENG device featuring a 4 cm^2 active layer area. The condition of the external force was 12 N and 20 Hz. In contrast, the unaltered TONC-PVDF TENG produced an open circuit voltage of 1.23 V, a short circuit current of 0.8 μA, and a maximal output power of 0.25 μW cm^{-2}. By substituting the pure cellulose film with the modified Alc/TONC film as the positive active layer, the corresponding Alc/TONC-PVDF TENG produced an open circuit voltage of 7.9 V, a short circuit current of 5.13 μA, and a maximal output power of 10.12 μW cm^{-2}. More specifically, the power density of the fundamental parameter output increased by approximately 41 times.[88] Undoubtedly, the execution of the TENG was substantially enhanced by the incorporation of NC.

2.2. Production methods of CNCs

Among the above discussed classes of NCs, CNCs find wide application in various fields like electronics, textiles, sensors, medical, and polymer-reinforced nanocomposites, which mainly results from the ease of producing surface functionalities and their self-assembly nature.[89] A brief about CNCs sources, crystalline properties, and preparation methods is summarized in Table 1. Despite their good properties, the dispersion of CNCs in the polymeric matrix remains a

Table 1 Description of CNC extraction processes, sources, yields, and crystallinity

Processes	Raw materials	Treatment procedures	Post-treatment	Yields (CPC to CNCs)	Crystallinity index	Ref.
Acid hydrolysis	Pigeon pea wood	4 N solution of HCl at 55 °C for 4 h	Quenching, dialysis, ultrasonication, and centrifugation	0.91	0.889	92
	Mustard straw	64 wt% H_2SO_4 at 55 °C for 30 min	Quenching, ultrasonication, centrifugation, and dialysis	0.82	0.827	74
	Bottle guard peels	64% (w/v) H_2SO_4 at 50 °C for 45 min	Dilution, dialysis, centrifugation, and ultrasonication	0.70	0.820	76
Enzymatic hydrolysis	Eucalyptus kraft pulp	Endoglucanase and xylanase or Cellubrix with endoglucanase at 50 °C for 72 h	Agitation, centrifugation, and ultrasonication	0.672–0.746	0.80–0.95	93
Ionic liquid treatment	Microcrystalline cellulose (MCC)	1-Butyl-3-methylimidazolium hydrogen sulfate and dimethyl sulfoxide treated at 90 °C for 60 min and then hydrolyzed for 30 min in deionized water	Quenching, sonication, and centrifugation	0.60	0.67	94
Subcritical water hydrolysis	Microcrystalline cellulose	MCC was filled with distilled water and then kept under pressure (8.1 MPa and 20.3 MPa) and at temperatures (120 °C and 200 °C)	Filtration, dialysis, and sonication	0.22	0.79	95

Open Access Article. Published on 08 Febwaliyo 2024. Downloaded on 12/09/2024 22:53:41.
This article is licensed under a Creative Commons Attribution-NonCommercial 3.0 Unported Licence.

challenge, which hinders the mechanical and electrical responses of the nanocomposites.[90] To avoid the agglomeration issues researchers have focused on the surface tailoring of the CNCs *via* hydrophobic modifications like silanes, metal oxides, and long carbon chain modifiers like surfactants, which resulted in good dispersion leading to their enhanced mechanical and electrical properties. For the production of CNCs, purification and pretreatment of cellulosic material are required through the extraction of hemicellulose, lignin, pectin, and waxes. CNCs are obtained through chemical extraction (acid hydrolysis).[78,91] The upcoming section deals with the various methods to fabricate the CNCs-based sensors and the methods to extract CNCs, followed by the sensing applications of CNCs-based probes.

2.2.1. Synthesis of CNCs. Various investigations have found that the physical, chemical, mechanical, and morphological qualities of CNCs change with the raw material source and extraction process. CNCs from natural sources are essential for pretreatment operations to remove lignin/hemicellulose/fat/waxes/proteins, *etc.* Naturally occurring cellulose has organized crystalline and disorganized amorphous areas. Thus, bulk cellulose is treated by chemical (acid hydrolysis), enzymatic, oxidative, mechanical, and green methods of hydrolysis to extract the crystalline portion.[96] A brief of morphology of CNCs synthesized by different processes is depicted in Fig. 1. Various CNCs extraction processes are discussed below sequentially:

Acid hydrolysis. This method is most widely used for CNCs extraction. It involves the diffusion of acid molecules into the amorphous region of cellulose. It is an acid-induced destructive process. Acids can release hydronium ions that penetrate the cellulosic chains and react with the oxygen elements, resulting in hydrolytic cleavage of glycosidic bonds in the amorphous part of the cellulose moiety.[96] After acid hydrolysis, the suspension is washed and rinsed, followed by dialysis in distilled water till pH neutralizes, indicating the removal of residual acid and neutralized salts. To get homogeneous CNC dispersion in an aqueous medium, sonication is done.

Acids employed to extract CNCs are sulfuric acid, hydrochloric acid (HCl), hydrobromic acid (HBr), phosphoric acid (H_3PO_4), maleic acid, hydrogen peroxide (H_2O_2), and a mixture of HCl and H_2SO_4.[70,75,102–105] Factors such as temperature, time of hydrolysis, concentration, and nature of acid play a crucial role in determining the characteristic properties of CNCs, namely crystal size, morphology, crystallinity, thermal stability, and mechanical and physicochemical properties.

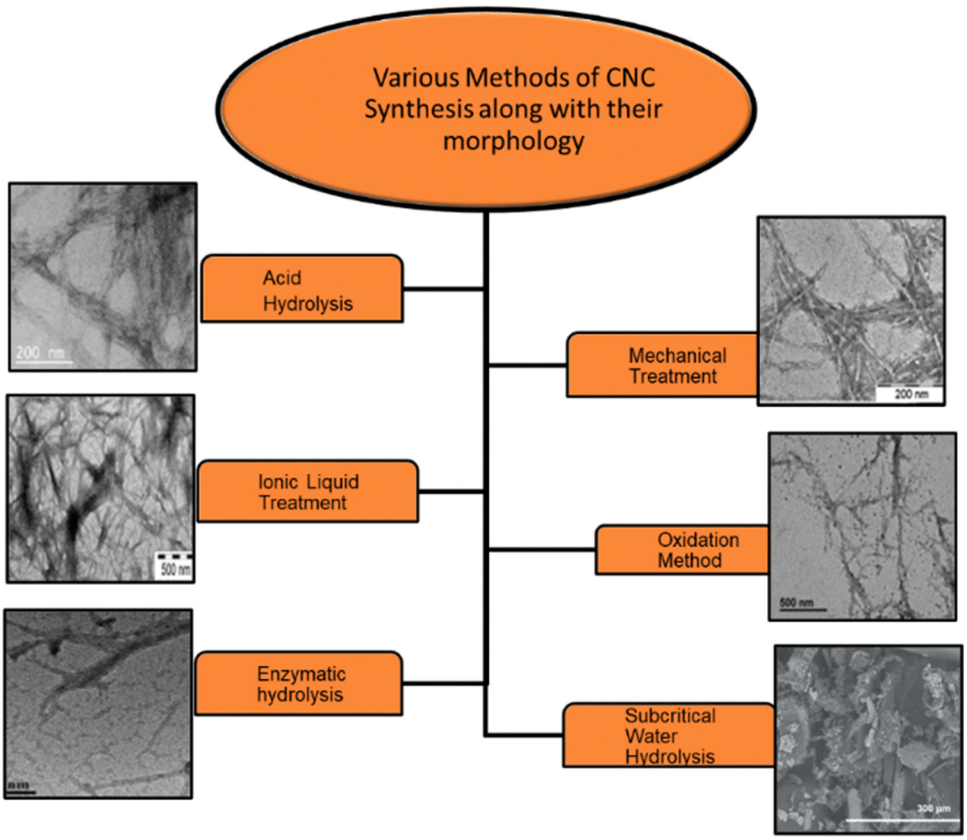

Fig. 1 Different types of methods employed to extract the CNCs from lignocellulosic mass and the respective morphologies.[92,97–101] Reproduced from ref. 97 with permission from ACS, copyright 2019. Reproduced from ref. 98 with permission from Elsevier, copyright 2015. Reproduced from ref. 99 with permission from Elsevier, copyright 2016. Reproduced from ref. 92 with permission from Elsevier, copyright 2023. Reproduced from ref. 100 with permission from Elsevier, copyright 2015. Reproduced from ref. 101 with permission from Elsevier, copyright 2015.

© 2024 The Author(s). Published by the Royal Society of Chemistry

Open Access Article. Published on 08 Febwaliyo 2024. Downloaded on 12/09/2024 22:53:41.
This article is licensed under a Creative Commons Attribution-NonCommercial 3.0 Unported Licence.

Mechanical treatment. Mechanical methods have also been extensively studied for the production of CNCs, either as a component of a fabrication process involving acid hydrolysis and oxidative and enzymatic treatments or directly. This treatment process is commonly used for the production of CNFs. It involves ultrasonication, microfluidization, and high-pressure homogenization.[106–113] Amin *et al.* have scaled up mechanical methods using high-energy bead milling (HEBM) to extract CNCs from aqueous or mild acid microcrystalline cellulose dispersions. This technique yields 57–76% CNCs with rod-like shape. CNCs have 85–95% crystallinity and strong thermal stability. Ultrasonication separates rod-shaped CNCs from MCC in water.[114] Through the ultrasonication method, production yield is less than 10%; hence, it is exempted.

Oxidation method. Apart from acid hydrolysis and mechanical treatment, CNCs can be prepared *via* the oxidation method. It involves oxidation of natural cellulose with the 2,2,6,6-tetramethylpiperidine-1-oxyl (TEMPO) radical followed by mechanical homogenization.[115] Reaction occurs on the surface and in amorphous domains of the cellulose fiber. The carboxylic group modifies the surface of CNCs through a direct ultrasonication-assisted TEMPO–NaBr–NaClO system. Due to anionic-charged electrostatic repulsion, carboxylated CNCs show better dispersibility in an aqueous solution. The amorphous part hydrolyzes gradually in this oxidation process, resulting in stable and well-dispersed aqueous suspension. Although the yield of CNCs obtained by this method is 80% with high crystallinity and high surface area, this method possesses severe drawbacks such as exploiting toxic chemicals (TEMPO reagents), thus leading to environmental problems and a long oxidation time.[116] Another reagent that is used for oxidation is periodate-chlorite. It is a two-step oxidation method in which periodate is initially utilized, followed by chlorite. However, it is a two-step, lengthy, and expensive process. Also, it causes disintegration of cellulose molecular chains by splitting glycosidic rings.

Green methods of CNCs production. The current trends are more focused on green and sustainable synthetic approaches. Taking this context, this section deals with the greener approaches towards CNCs production. We have categorized such approaches into five types as follows: (a) enzymatic hydrolysis, (b) ionic liquids, (c) deep eutectic solvents, (d) electron beam irradiation, and (e) subcritical water hydrolysis. In some reports, the oxidation method has also been termed as the green method for the CNCs extraction, which we have already discussed.

(a) Enzymatic hydrolysis. Enzymatic hydrolysis is an economically viable alternative that avoids the usage of harsh chemicals and lessens energy consumption. Enzymes selectively digest amorphous domains of cellulose, resulting in CNCs that maintain hydroxyl group surface chemistry, enabling more straightforward chemical modification. Cellulase is a mixture of endoglucanases, exoglucanases, and cellobiohydrolases, mainly used to catalyze cellulose hydrolysis. These three entities act synergistically.[117] Endoglucanase randomly attacks to hydrolyze amorphous regions, whereas exoglucanase reacts with reducing or non-reducing ends and cellobiohydrolase hydrolyzes from either the C1 or C4 end of the cellulosic chain.[118] Cellobiohydrolases tend to penetrate both amorphous and crystalline regions. However, some challenges of this procedure are the cost and availability of enzymes, longer processing time causing cellulose degradation, and less yield that can be improvised by pretreating in DMSO or NaOH.[119]

(b) Ionic liquid (IL) treatment. There are multiple ways to prepare CNCs apart from these methods. Recently, ionic liquids have been utilized to extract CNCs due to their peculiar solvating properties for material processing. IL treatment is highly optimized for cellulosic hydrolysis for the isolation of nanoparticles.[94] For CNCs extraction purposes, imidazolium-based acidic ILs, such as 1-ethyl-3-methylimidazolium diethyl phosphonate ([EMIM]DEP), 1-butyl-3-methylimidazolium chloride ([BMIM]Cl), 1-butyl-3-methylimidazolium acetate ([BMIM]OAc) and 1-butyl-3-methylimidazolium hydrogen sulfate ([BMIM]HSO_4), are exclusively used as solvents. Imidazolium ILs involve the selective dissolution of amorphous zones while conserving the native conformation of cellulose type I. Mao *et al.* developed a two-step hydrolysis approach using [BMIM]HSO_4 in which MCC is allowed to swell at room temperature, followed by hydrolyzing it at 100 °C for about 12 h. This procedure yields a high CNCs content of up to 76% along with good surface properties of CNCs.[120] Nevertheless, ionic liquids are not without their limitations, making it difficult to recommend them as an entirely environmentally friendly substitute for acid hydrolysis. Ionic liquids incur higher production costs due to their potentially hazardous synthesis procedures, noxious properties and lower recovery rates.

(c) Deep eutectic solvents. Deep eutectic solvents (DES) are eutectic mixtures composed of Brønsted or Lewis bases and acids. DESs are easily generated through the thermal combination of a donor and acceptor pair of hydrogen bonds that are capable of forming a eutectic composite. Because of the ease and safety of their synthesis, DESs are considered ecological solvents. Certain DESs have demonstrated biodegradability as well.[121] Due to the chemical similarity between DESs and ionic liquids, DESs can be utilised in lieu of ionic liquids in a variety of applications, including the production of CNCs. This eliminates the two primary drawbacks of ionic liquids, which are their high cost and toxicity. DESs have the potential to be utilised as straightforward and environmentally friendly agents for extracting CNCs. Analogous to ionic liquids, DESs facilitate the reaction by functioning as both solvents and catalysts. Significantly, the reaction conditions employed in the isolation of CNCs are typically moderate, and the DESs can be recovered through distillation five times with a recovery rate exceeding 80%.[122] Nevertheless, as previously stated in the section on ionic liquids, the industrial scale recovery rate and reaction cycles continue to be obstacles.

Open Access Article. Published on 08 Febwaliyo 2024. Downloaded on 12/09/2024 22:53:41.
This article is licensed under a Creative Commons Attribution-NonCommercial 3.0 Unported Licence.

(d) Electron beam irradiation. A more obscure green method, electron beam irradiation, has also been described in the literature. By employing a two-step methodology involving electron beam irradiation (EBI) and high-pressure homogenization, Lee *et al.* synthesized rod-shaped CNCs from dissolved softwood fibre. By reducing the degree of polymerization facilitated by EBI, CNCs could be extracted without the requirement of strong acid hydrolysis.[123] The literature is very limited on this method.

(e) Subcritical water hydrolysis. Super and subcritical water has lower ionization constant (K_w) values with higher concentrations of ionized species like water molecules and hydronium ions (H_3O^+), which assist in efficient hydrolysis. There have been some reports where the subcritical water hydrolysis method is employed for CNCs preparation. Subcritical water hydrolyzes the cellulose, maintaining 120 °C temperature and 20.3 MPa pressure for 60 minutes. The advantage of this process involves utilizing water as a reagent, which is a green source, cheap, and yields lesser and cleaner effluents. Also, suspension shows higher diffusivity, activity, and easy ionization, and only around 22% yield was obtained under these hydrolysis conditions. CNCs obtained by this process offer a high crystallinity index of approximately 79%, having a similar rod-like morphology and aspect ratio to those of conventionally extracted CNCs.[95,124]

2.3. Structural arrangement of CNCs and their properties

Researchers are inclined toward investigating natural and sustainable nanomaterials that possess fascinating properties when used for reinforcing and for many other applications. One such nanomaterial is CNCs, which possesses numerous peculiar and versatile properties that make it suitable for various applications, as shown in Fig. 2. The main cause of CNCs having such properties is their self-assembly behaviour.

Subsequent research revealed that, above a certain concentration threshold, these rod-shaped nanocrystals generate colloidal suspensions that are stable, thereby facilitating the self-assembly of the crystalline nanorods of CNCs in the absence of external interference.[125] In the equilibrium state, these CNCs suspensions show biphasic behaviour, which consists of isotropic and liquid crystalline (LC) domains. Upon raising concentration, the shift from a LC state to a gel state is caused by the enhanced interparticle interactions. A further increase in concentration leads to complete LC ordering, resulting in inhibition of the isotropic phase. These enduring suspensions serve as illustrations of anisotropic (LC phase) deformable lignocellulosic nanomaterials. The self-assembly (LC phase), alternatively referred to as the chiral nematic (cholesteric) phase, is distinguished by the anisotropic long-range arrangement of cellulosic chains at the macroscopic level. Therefore, CNCs suspensions demonstrate lyotropic LC behaviour spontaneously. Polarised optical microscopy (POM) and circular

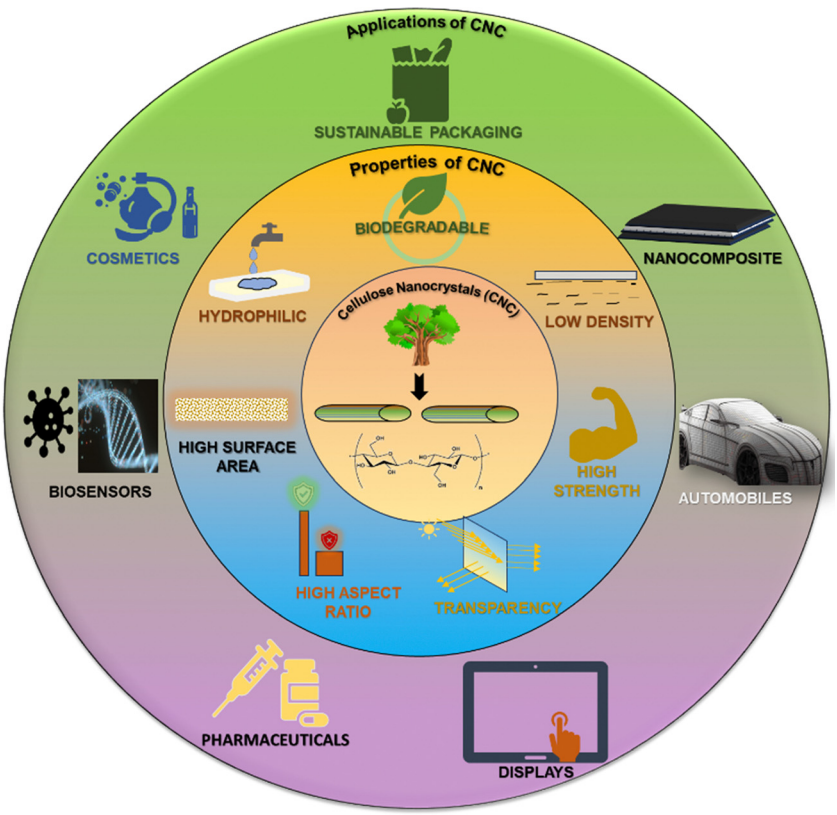

Fig. 2 The CNC properties and its application in versatile fields.

© 2024 The Author(s). Published by the Royal Society of Chemistry

Open Access Article. Published on 08 Febwaliyo 2024. Downloaded on 12/09/2024 22:53:41.
This article is licensed under a Creative Commons Attribution-NonCommercial 3.0 Unported Licence.

dichroism (CD) spectroscopy provide evidence that chiral LC state formation takes place above a critical concentration (dependent on the CNC's properties).

The director (n), which represents the standard orientation and long-range organisation of chains, is promoted by the CNC rods' high aspect ratio. The helical arrangement of the director (m) occurs when cellulose molecules align due to their inherent chirality.[126] The CNCs helix exhibits a consistent leftward orientation as a result of the chirality inherent in the nanorod organisation. Pitch p is the distance alongside the helical axis that separates the CNCs nanorods following a 360° rotation (a complete helical fold). The ultimate refractive index fluctuates intermittently as a result of the spiral configuration of nanorods; each successive layer transforms the substance into a self-assembling birefringent crystal.[127] The wavelength of the reflected light from such chiral nematic arrangements is given by eqn (1)

$$\lambda_{max} = n_{avg} p \sin(\theta) \quad (1)$$

where the de Cries wavelength is λ_{max}, θ is the angle at which the incident light falls on the respective crystal, n_{avg} is the average refractive index (characteristically 1.54 for the CNCs), and p is the length of formed helix termed as pitch.[128] Pitch values in the aqueous medium range from a few tens of micrometres. Thin CNCs films are formed by the suspensions themselves following prolonged evaporation. When the pitch is reduced to the submicron scale, it manifests to the unaided eye as iridescent hues.[129–131] The chiral nematic phase, which is generated through the arrangement of mesogenic units, demonstrates birefringence and can be identified using POM as a distinctive fingerprint region. The ability of these lyotropic liquid crystals to keep their self-assembly even after the aqueous medium is removed is a critical parameter. This facilitates the production of synthetic substances that possess unparalleled optical characteristics. VASA and EISA, which stand for vacuum-assisted self-assembly and evaporation-induced self-assembly, are the two most prevalent methods for producing solid films.[132,133] While EISA is the method most frequently employed, it is a laborious procedure that frequently results in the observation of polydomain structures in the desiccated films due to the heterogeneity of the evaporation rate. Conversely, VASA yields iridescent coatings that are more homogeneous in nature, devoid of any discernible ''coffee stain'' rings.[134]

Biodegradable CNCs can be used as sustainable packaging materials, agricultural film wraps, covers, biomedical implants, and dressings.[135] Also, biopolymers like myrcene have been also explored in the field of packaging.[136] Low-density or lightweight CNCs find application in nanocomposites and thermal insulating materials for construction purposes. A polymer matrix reinforced with CNCs shows high mechanical strength and is thus used in aerospace and automotive industries.[137] CNCs are optically active and transparent and so they can be used as optical films for touchscreen displays, eyewear, window coatings, and wearable electronics. CNCs possess a high aspect ratio (*i.e.*, a high length : breadth ratio) and are hence used for reinforcement and incorporated with paper and cardboard, polymers, plastics, rubber, *etc.*[138–142] to improve structural performance and longevity while reducing weight simultaneously. High aspect ratio CNCs shows good film-forming ability and is therefore used as a thin transparent barrier film for packaging and flexible electronic components. The increased surface area of CNCs leads to enhanced interactions and functionalities that control the efficient release of drugs from targeted drug delivery systems. These properties also result in a significant material potentially being used as a stimuli-responsive sensor. The large surface area of CNCs enriches cell growth and adhesion, facilitates wound healing and tissue engineering scaffolds, and enables the removal of contaminants and toxins from liquids and gases through adsorption and is utilized in water purification and air filtration applications. CNCs are hydrophilic in nature, and they are suitably used for cosmetics and personal care, drug delivery, and wound care. They can be used as water filtration membranes and promote adsorption and removal of water-soluble contaminants. This section discussed about the structural arrangements, properties and the applications of CNCs. The upcoming sections will deal with the utility of CNCs in the sensing applications, the historical development of CNC based sensors, their fabrication methods, and their classification.

3. History of CNCs in sensing

The development of sensing technology throughout history has been quick, and systematic advancement has accelerated exponentially over the past few decades. Biosensors are no longer restricted to detection by the electrochemical response but can also run *via* piezoelectric, optical, and thermal mechanisms. Since their introduction in 1956, biosensors have become widespread in food technology, clinical diagnostics, forensic analysis, environmental studies, and drug development.[143] While the first class of biosensors were electrochemically responsive in nature, advanced biosensors have expanded their detection mechanisms to include optical, piezoelectric, and many others. The objective of extending a new category of sensors is to use a sustainable method for sensor construction and eco-friendly materials, like nanocellulose.

Nanoscale cellulose has a high catalytic efficiency, high surface area, robust adsorption capability, and high surface area activity. As a result of these enhanced properties at the nanoscale, it becomes a crucial material for sensors. The advancement of nanocellulose-based sensing platforms has taken their accomplishments in this field into account. The first report on cellulose-based sensors was made by Southern in 1975. His report described the sensing of specific DNA fragments using cellulose nitrate filters.[144] This gives an inference that cellulose is a candidate established long ago as a sensing probe. This review explicitly addresses the sensing application of CNCs as sensing probes. Here, we have covered the development of CNCs-based sensors in the last decade.

Open Access Article. Published on 08 Febwaliyo 2024. Downloaded on 12/09/2024 22:53:41.
This article is licensed under a Creative Commons Attribution-NonCommercial 3.0 Unported Licence.

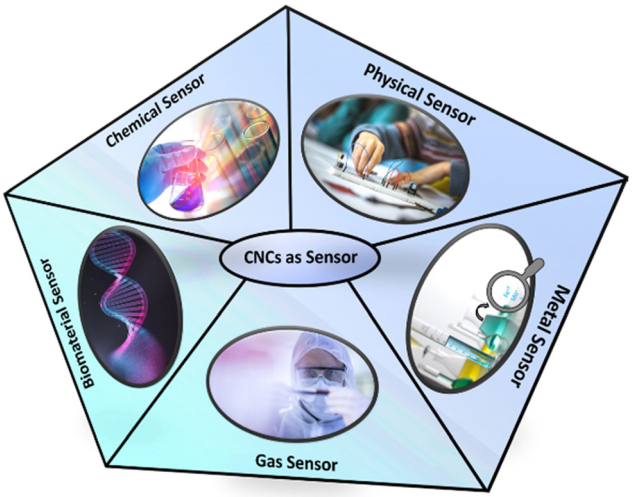

Fig. 3 Application of CNCs as sensing probes.

Fig. 3 shows the development of the CNCs-based sensors for metals, gases, chemicals, physical stimuli, and biomaterials. Additionally, Fig. 4(a) and (b) illustrates the progressive growth of research in the domain of CNCs-based sensors over the previous decade. Strings ''sensors'' and ''cellulose nanocrystals'' were used on SciFinder^{n} within the reference search, and ''Cellulose Nanocrystal based sensors'' to get an idea about the development of the research interest in this field. The string provides information that 5494 publications were published between 1975 and 2024. The results were 3938 when refined to the previous decade, 2014–2023. This indicates that approximately 71.68 percent of the publications were done in the preceding decade. This unequivocally demonstrates that interest in this field has grown significantly over the past decade and that the significance of sensors based on CNCs has increased substantially.

Schyrr *et al.*[19] developed functionally enhanced surface-area scaffolds derived from CNCs and poly(vinyl alcohol). This platform aids fluorescence-based sensing. The approach was improved to detect protease action by arresting the Förster-type resonance energy transfer chromophore pair through a labile peptide sequence to the scaffold.[145] Overall, they have demonstrated the possible pH-sensitive sensing probes for monitoring wound fluid, which is directly applicable in real-time for medical applications. Sadasivuni *et al.* reported one more deal-breaker development. They presented an eco-friendly and transparent sensor made by the spraying method on modified graphene oxide-filled CNCs on lithographic designs of interdigitated electrodes on polymer substrates to locate approaching objects in 2014. Their finding has established that sensing based on CNCs is not limited to basic sensing applications; they can be further explored in high-end sensors like proximity sensors. Chen and colleagues[146] revealed promising biomedical and inorganic nanoparticle encapsulation applications using poly(amidoamine) (PAMAM) dendrimers in 2015. Such hybrids can be used in pH-responsive nanodevices, fluorescence-based pH sensors, optical indicators, and nanoreactors for inorganic nanoparticle encapsulation due to their pH-responsive and fluorescence features. The suggested methodology can be used in any field of detection and sensing where changes are in a wide range. In 2016, new developments of CNCs-based sensors were made, with one of them by Wu and co-workers.[147] They developed a sandwich-structured cellulose nanocrystal-based nanocomposite photonic screen to resemble Chrysina beetle shells. The suggested self-assembled photonic material is interesting for application as an optical anti-counterfeiting film, a tunable bandpass filter, a reflector or polarizer, and a humidity-responsive actuator. Another report published in 2016 by Cao *et al.*[148] provides a green assembly method for making natural rubber (NR) composites with 3D organized graphene-based conductive complexes. This unique 3D conductive network gave the NR composites improved mechanical characteristics, electrical conductivity, and resistivity response to organic liquids. Their method for making liquid sensors for chemical industry solvent leakage detection and environmental monitoring was

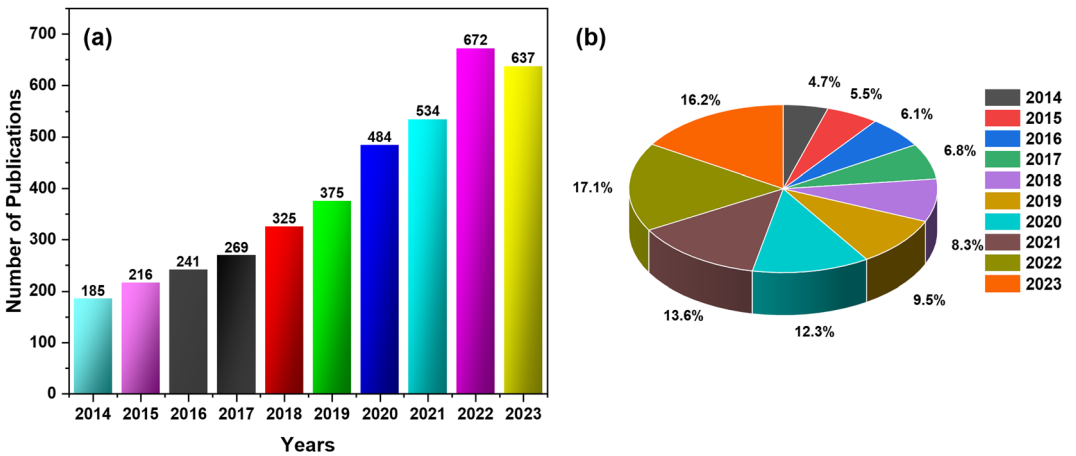

Fig. 4 Statistical analysis of research publications between 2014 and 2023 using string ''Cellulose Nanocrystal based sensors'' on SciFinder^{n} on 20th Dec 2023. (a) Yearly distribution of the number of publications between 2014 and 2023, and (b) year wise percentage contribution of research efforts on CNCs-based sensors (a pie chart).

© 2024 The Author(s). Published by the Royal Society of Chemistry

Open Access Article. Published on 08 Febwaliyo 2024. Downloaded on 12/09/2024 22:53:41.
This article is licensed under a Creative Commons Attribution-NonCommercial 3.0 Unported Licence.

unique, simple, and eco-friendly. Dai *et al.*[149] addressed gas sensing, which emerged with industrialization. They studied the structure, optical, and sensing properties of an ammonia gas sensor established on cholesteric liquid crystal based films of copper(II)-doped CNCs. Such a hybrid film enhanced a new gas detection regime for rapid and efficient qualitative investigations. Wu and his colleagues[150] proposed dye-loaded CNCs for ionic strength and solvent detection in 2018. They created fluorescent and stimuli-responsive CNCs by covalently coupling a 1,8-naphthalimide dye to TEMPO-oxidized CNCs. Due to the unique aggregation-enhanced emission (AEE) effect, fluorescent CNCs are promising nanomaterials for various sensing applications like ionic strength and solvent polarity. Han *et al.*[151] reported polypyrrole-coated CNCs films using iron chloride ($FeCl_3$) as an oxidant to reinforce polyvinyl alcohol (PVA) in 2019, which shifted the focus of CNCs-based sensors towards self-healing skin sensors. These nanocomposites have superior sensing properties for real-time monitoring of large and subtle human motions (swallowing, finger bending motions, and wrist pulse); consequently, they have significant applications in flexible skin sensors, health monitoring, and wearable electronic devices. In the year 2020, Ivan and his colleagues[152] established that the structural characteristics of CNC-patterned tin dioxide films are highly dependent on the composition of the precursors. The sensor exhibits highly selective sensitivity to carbon monoxide (CO) in ppm (parts per million) concentrations and minimal cross-sensitivity towards humidity. This research introduced a new dimension for detecting gases using sensors based on CNCs. Ye *et al.*[153] described novel rhodamine-based fluorescent CNCs (RhB-CNCs) as an efficient colorimetric and fluorescent sensor for detecting Hg^{2+} in aqueous solutions. They established that fluorescently labeled CNCs are readily applicable for the selective and sensitive detection of Hg^{2+} in aqueous medium and have enormous capability for use in bioimaging, chemosensing, and effluent treatment. In 2021, CNCs-based 3D printable sensors came into the picture; Lai and his colleagues[154] prepared 3D printable CNCs composites with Al^{3+} and zwitterionic hydrogels for wearable electronics and sensing. Additionally, 3D printing facilitated the design of tactile sensors with improved sensitivity. By exploiting the surface functionality of the nanocrystals, their nanocomposite hydrogels attained high transparency, excellent mechanical strength, and 3D printability simultaneously. Sun *et al.* (2022)[155] have reported iron sensing, specifically Fe^{3+}. 7-Amino-4-methylcoumarin (AMC) and decarboxylated CNCs (DCN) underwent successive periodate–chlorite oxidation to produce fluorescent dicarboxylic CNCs (FDCN) with selective quenching of Fe^{3+}. Due to FDCN's high sensitivity, hydrophilicity, and selectivity for Fe^{3+}, the chemosensor is appropriate for Fe^{3+} trace sensing in water used for drinking and biological aspects. Recently, in 2023, Fan and his coworkers[86] reported CNCs/polyaniline (PANI) composite films that respond to stimuli for use in optical and electrochemical detection. A self-assembly procedure was optimised to produce CNCs–PANI and CNCs–glucose–PANI based films with a vibrant colour. A two-layer, conductive CNCs–PANI based film was fabricated and integrated into an electrical circuit, where it could function as a chemical warning alarm for supervising the environmental and reaction conditions. This unique iridescent CNCs–PANI based film displays the potential for detectable electrochemical multi-sensing by using eco-friendly, natural substances.

The above section summarized how the evolution of CNCs-based sensors has occurred from 2014 to 2023. Various research groups have exploited them for different sensing applications. It started with wound pH monitoring and covered gas, metal, protein, wearable, and optical and electrochemical sensors. The field is vibrant and not limited to these sensing applications. Many sensing probes can be developed and utilized for versatile fields like chemical industry, pharmaceuticals, food packaging, supply chain, and water management.

3.1. Fabrication of CNCs based sensors

It is becoming increasingly crucial to fabricate such sensors, and many studies detail various production methods. The most common approaches for the manufacturing process are listed out below.

Such sensors can be made by compression molding as SBS/CNCs/CB-based composite sheets were prepared by Huang *et al.* for strain sensing.[156] In another methodology reported by Li *et al.* EISA-assisted tunicate CNCs/PVA films were prepared, and their sodium alginate-based hydrogels were prepared for calcium ion sensing in sweat.[157] Li *et al.* have reported a free radical copolymerization method to prepare CNCs-based sensing probes. They used these sensors for strain response monitoring.[158] Wei and co-workers have reported humidity sensors based on CNCs. They used the solution casting method to prepare such humidity-responsive CNCs-based composite films.[159] In another report, GO@CNCs nanocomposites were prepared for acetone sensing by Orasugh *et al. via* a slurry method.[160] Verma *et al.* reported layer-by-layer EISA-assisted CNCs-based humidity sensors.[7] These are some recent reports where different methods have been used to fabricate CNCs-based sensors for humidity, chemical, gas, sweat, and metal ion sensing. The detailed construction and classification of such sensors are described in the upcoming sections on metal, gas, chemical, physical stimuli, and biomaterial sensing.

4. Classification of CNCs based sensors and their recent advancement

This section deals with the classification of CNCs based sensors. Such sensors can be classified into metal, gas, chemical, physical stimuli, and biomaterial sensors. Their subcategories have also been discussed in detail.

4.1. Recent advances in CNCs-based sensors for metal sensing

Metals are essential for human lives, but up to a certain level of concentration. Increased intake of hazardous metals can lead to death and adversely affect health. That is why metal

Open Access Article. Published on 08 Febwaliyo 2024. Downloaded on 12/09/2024 22:53:41.
This article is licensed under a Creative Commons Attribution-NonCommercial 3.0 Unported Licence.

contaminant detection is a requirement, which should always start with figuring out where the contamination could be induced in a system. This is where metal detection comes into the picture. Functionalized CNCs with ligands or compounds with a significant affinity for particular metal ions can behave as sensors for metals and their detection in solvent media. These functional groups can selectively bind to the metal ions of interest, resulting in additional alterations to the properties of CNCs. For instance, when functionalized CNCs come into contact with metal ions, they may undergo color changes, fluorescence changes, or electrical conductivity modifications. In metal ion detection systems, CNCs can function as signal transducers. This indicates that CNCs can be incorporated into sensing platforms, such as composite materials or nanosensors, in order to detect the presence of metal ions. Changes in the properties of CNCs upon interaction with metal ions provide a straightforward and efficient method for determining and detecting the presence and concentration of the target metal ions. A few examples of sensing metals, like iron and mercury, are shown in Fig. 5. This attribute makes CNCs ideal candidates for the development of efficient metal ion sensing technology.

For the purpose of finding lead ions in a completely aqueous solution, a fluorescent probe has been created by Song and his colleagues.[163] The 1,8-naphthalimide fluorescent dye is chemically bonded to CNCs to produce this sensing probe. The CNCs

Fig. 5 Use of CNCs in metal sensing: (a) tannic acid loaded CNCs for Fe^{3+} detection[161] and (b) bovine serum albumin-protected-gold-nanocluster (Au@BSA NC) loaded CNCs–alginate hydrogel beads.[162] Reproduced fsrom ref. 161 with permission from Elsevier, copyright 2021. Reproduced from ref. 162 with permission from ACS, copyright 2016.

© 2024 The Author(s). Published by the Royal Society of Chemistry

Open Access Article. Published on 08 Febwaliyo 2024. Downloaded on 12/09/2024 22:53:41.
This article is licensed under a Creative Commons Attribution-NonCommercial 3.0 Unported Licence.

that have been dye-modified have multiple carboxyl and hydroxyl groups on their surface, which help them disperse well in water. While the 1,8-naphthalimide dye alone does not show appreciable variations in fluorescence when exposed to different metal ions, the CNCs with the dye show a particular and sensitive reaction to lead ions (Pb(II)), resulting in a marked rise in emission intensity. At 1.5×10^{-7} mol L^{-1}, the detection limit of these fluorescent CNCs is very low. Additionally, a significant linear relationship occurs between the maximum fluorescence and Pb(II) concentration throughout a wide range, from 2.5×10^{-7} mol L^{-1} to 5.0×10^{-5} mol L^{-1}. The combination interaction of Pb(II) with the grafted dye groups and the adjacent carboxyl groups on the surface of the CNCs is thought to be the cause of the dye-labeled CNCs' capacity to detect Pb(II). It was discovered through experimentation that the ratio of Pb(II) to the fluorophore on the CNCs is roughly 1.2 : 1, closely matching the theoretical ratio of 1 : 1 according to Job's plot experiment. These fluorescent CNCs could be used as nanosensors to find different metal ions. They have developed a material with great sensitivity and selectivity in identifying and measuring lead ions; such materials have the potential to be used in chemical, environmental, and biological systems.

Hanif *et al.*[161] have also developed a sensing platform for Fe^{3+} ions; in this work, they have used tannic acid (TA) covalently bonded to the surface of CNCs to produce TA@CNCs, a nanohybrid material. The TA@CNCs nanohybrid was applied to a variety of surfaces with qualities ranging from flexible to rigid and hydrophobic to hydrophilic in a water-based dispersion form. This was accomplished *via* a straightforward drop-casting procedure. The coated TA@CNCs demonstrated a strong ability to detect Fe^{3+} ions in a variety of liquids, including milk, serum, and water, in a selective and sensitive manner. The coated TA@CNCs underwent a substantial color shift in the samples, turning from light gray to black after coming into contact with Fe^{3+} ions. For serum samples and milk samples, the limit of detection (LOD) values for detecting Fe^{3+} were discovered to be 0.52 ppb and 0.54 ppb, respectively. The color shift and the detection limit show that the coated TA@CNCs nanohybrid is capable of detecting traces of Fe^{3+} ions. This method's novel feature is the coating of TA@CNCs onto multiple substrates, which can offer a scalable, simple, and economical way to create a portable sensing platform to detect Fe^{3+}, as depicted in Fig. 5(a). This technique shows promise because it is highly biocompatible and has a wide range of possible uses.

There was one more report on fluorescent CNCs by Zhang and co-workers.[164] They investigated the potential of fluorescent cellulose nanocrystals (fCNCs) as optical probes for uses such as bioimaging and metal ion detection in their study. The surface of CNCs was altered through a controlled esterification procedure applying ethylenediaminetetraacetic dianhydride (EDTAD) to produce high carboxylation levels while maintaining surface integrity and crystalline structure. A variety of fCNCs with various densities of fluorescent 7-amino-4-methylcoumarin (AMC) were created by altering the carboxylation levels. Because of the steric effects of AMC molecules on the fCNCs surface, self-quenching was reduced, resulting in more stable fluorescence, which, even in solid form, was consistent with changes in fCNCs concentration. Under UV light, fCNCs' fluorescence preferentially changes from blue to purple as a result of the presence of copper ions (Cu^{2+}). This makes it possible to measure the concentration of Cu^{2+} using two linear correlations: the fluorescence intensity ratio of 440 nm to 390 nm within 16–160 ppm Cu^{2+} and the fluorescence attenuation ratio at 390 nm within 0.5–16 ppm Cu^{2+}. The fluorescence of the prepared material (fCNCs) matched the specifications of the World Health Organization's Guideline of Drinking-Water Quality (GDWQ) at a crucial Cu^{2+} concentration of 0.5 ppm. This method can be applied for a quick and visual evaluation of drinking water quality. This work created a new fluorescent nanomaterial for metal ion detection.

Zahang *et al.*[165] converted CNCs into fluorescence-labeled nanoparticles (referred to as Py-CNCs) through a three-step process. The fluorescence emission was improved when CNCs were modified with pyrene. When tested for their capacity to detect metal ions, the Py-CNCs nanoparticles strongly prefer Fe^{3+} detection over other screening metal ions. Additionally, they effectively distinguish between Fe^{2+} and Fe^{3+} ions. Across a wide range of concentrations, Py-CNCs exhibit remarkable selectivity for Fe^{3+} ions, which is seen by released variations in the light spectrum. This sensing-capable nanomaterial reported by them has potential uses in several areas, including chemistry, environmental monitoring, and biological systems.

Mohammed *et al.*[162] developed a novel system composed of CNCs and customized luminous metal clusters. Bovine serum albumin ideally structures and protects these metal clusters. Beads made of the cellulose nanocrystal–alginate hydrogel contain them. Heavy metal ions can be detected and eliminated by this technology, with a concentration of mercury ions found in water. Their idea also offers a novel method for observing how these heavy metal ions disperse inside the hydrogel beads. This is accomplished by monitoring variations in the fluorescence of metal clusters (Au@BSA NCs) as they interact with mercury ions throughout the diffusion process, as shown in Fig. 5(b). This method may be used to determine the effective diffusion coefficient for these heavy metal ions in the hydrogel beads. This work reported the detection and the removal of heavy metals.

The above section described the evolution of CNCs-based metal sensors and how the CNCs-based sensing probes can selectively detect a specific metal. Mainly, the fluorescence, dynamic light scattering, pH, and optical adsorption methods have been used for the identification of metals using CNCs based composites, which were fabricated by either chemical modification or by physical mixing with the stimuli responsive materials. Table 2 describes some other essential reports on metal sensing achieved using CNCs-based sensors.

4.2. Recent advances in CNCs-based sensors for gas sensing

Leakage of hazardous, toxic, and polluting vapors is one of the most common accidents that occur during the chemical manufacturing process, and it is extremely dangerous to the health

Open Access Article. Published on 08 Febwaliyo 2024. Downloaded on 12/09/2024 22:53:41.
This article is licensed under a Creative Commons Attribution-NonCommercial 3.0 Unported Licence.

Table 2 NC-based biosensor probes for metal sensing

S. no.	CNCs nanocomposites	Sensing methods	Metals detected	Detection limits	Ref.
1	1,8-Naphthalimide dye with CNCs	Fluorescence	Pb^{2+}	2.5×10^{-7}–5.0×10^{-5} mol L^{-1}	163
2	PDA@CNCs	Dynamic light scattering method	Fe^{3+}	0.5 ppm 3 ppm (naked-eye)	166
3	CF-CNCs	Fluorescence	Fe^{3+}	0–50 μM	167
4	CNCs–SA–$COOC_6$TPP	Ratiometric fluorescence chemosensing	Hg^{2+}	0.05 μM	168
5	$CNCs_{SL}$, $CNCs_{BE}$ or $PCNCs_{SL}$	pH and FESEM	Ag^{+} and Cu^{2+}/Fe^{3+}/Fe^{2+}	(5.0–6.1 μM)	169
6	CNCs–EDTAD–AMC	Fluorescence	Cu^{2+}	0.5 ppm	164
7	Py-CNCs	—	Fe^{3+}	1×10^{-6} M	165
8	(Au@BSA NC)-loaded CNCs	Batch adsorption experiments	Hg^{2+}	—	162
9	(RhB–CNCs)	Fluorescence	Hg^{2+}	232 nM	153
10	CNCs and polyethyleneimine capped-silver clusters	Fluorometric sensing	Cr^{6+}	0–400 mg L^{-1}	170

of human kind. Taking this into context, studies have shown that real-time monitoring of the gases is advantageous for warning of hazardous gases and malfunctioning protective equipment at disaster and accident sites. With the growing prevalence of flexible wearable devices, portable intelligent terminals that exhibit exceptional electrical and optical performances and high integration have risen to prominence in academia and industry.[171] However, most gas sensors are comprised of rigid base materials, such as ceramics and quartz, which limits their application in wearable devices. Moreover, high polymeric substances, such as polyimide (PI), polyethylene naphthalate formic acid ethyl ester (PEN), and poly diethyl terephthalate (PET), have been utilized as flexible substrates in gas sensors due to their quality and bending characteristics.[172] However, these materials cannot be degraded naturally and have weak anti-aging and thermal stability. In recent years, CNCs have been progressively applied as biosensors, and it is believed that their properties can also be applied to the research of gas sensors. As a biodegradable natural cellulose nanomaterial, the physicochemical properties of CNCs are beneficial for producing flexible, transparent, and strong substrate films for wearable gas sensors.[173] Fig. 6 shows the use of CNCs in gas sensing.

In a study reported by Zhao *et al.*[174] they made a chiral nematic CNCs film that reacts with two separate inputs. The iridescent chiral nematic CNCs film could reverse its motion in response to humidity and formaldehyde gas variations. The color of the CNCs iridescent film changed noticeably by the creation of hydrogen bonds, and its response range was 165 nm when the relative humidity (R_H) was raised from 43 to 99%. Due to the existence of these hydrogen bonds, the CNCs iridescent film displayed a response range of 98 nm for the formaldehyde-gated behavior when the concentration of formaldehyde gas was raised from 0.14 to 14 mg m^{-3}. However, a normal human eye could not detect the color shift. Through the formation of physical cross-linking networks by hydrogen bonds between water, formaldehyde, and CNCs, it was discovered that the interaction between the humidity response and the formaldehyde response was a synergistic effect of cooperation and competition between water and formaldehyde molecules. Overall, this study infers that the chiral nematic structure of CNCs can show multi-stimuli behavior and can be used to manufacture sensing devices. Fig. 6(a) shows the EISA-assisted CNCs films as humidity and formaldehyde gas sensors.

In another report, Ivanova *et al.*[152] described a flexible method for employing CNCs to help fabricate nanostructured tin dioxide thin films. They showed that achieving extremely porous, thin films with pore sizes ranging from 10 to 20 nm is feasible by optimizing the precursor conditions to produce homogenous precursor mixtures. Finally, a resistive gas sensor based on the tin dioxide CNCs-template using the material's large surface area is created. Tin dioxide is classified as an n-type semiconductor and is widely recognized as a crucial material in the production of resistive gas sensors. The electronic conductivity of tin dioxide is significantly influenced by surface-chemical reactions with gas molecules that either reduce or oxidize. Therefore, the measurement of ohmic resistance enables monitoring the presence of these gases at low parts per million (ppm) concentrations. The preparation of the porous film in its original location results in a sensor device that exhibits a robust mechanical connection between the CNCs and tin oxide and reliable electrical contact with the electrodes. The obtained porous layer demonstrates nanocrystalline characteristics, with an average grain size of 9 nm. This nano-crystallinity is advantageous, as it contributes to the high performance of the sensor. The sensor has a low cross-sensitivity to humidity and an increased sensitivity to carbon monoxide (CO) in ppm concentrations. Hence, from this report, it can be concluded that CNCs can be used as bio-inspired templates to form porous films that can be used as gas sensors.

Song *et al.*[175] created colorimetric sensors that are able to change their color when confronted with aldehyde vapors. They modified CNCs using 3-aminopropyltriethoxysilane, which was then used to make amine-functionalized CNCs. The CNCs films underwent chemical and physical changes, such as swelling, when aldehyde gases interacted with the amine groups due to the formation of crystalline arrangements. The end result was a color shift that was visible to the human eye at high concentrations and could be captured by digital cameras at levels as low as parts per million. Fig. 6(b) shows the mechanism of CNCs-based sensor preparation and its working mechanism. Fig. 6(c) establishes the colorimetric response of the prepared formaldehyde gas sensor.

© 2024 The Author(s). Published by the Royal Society of Chemistry

Open Access Article. Published on 08 Febwaliyo 2024. Downloaded on 12/09/2024 22:53:41.
This article is licensed under a Creative Commons Attribution-NonCommercial 3.0 Unported Licence.

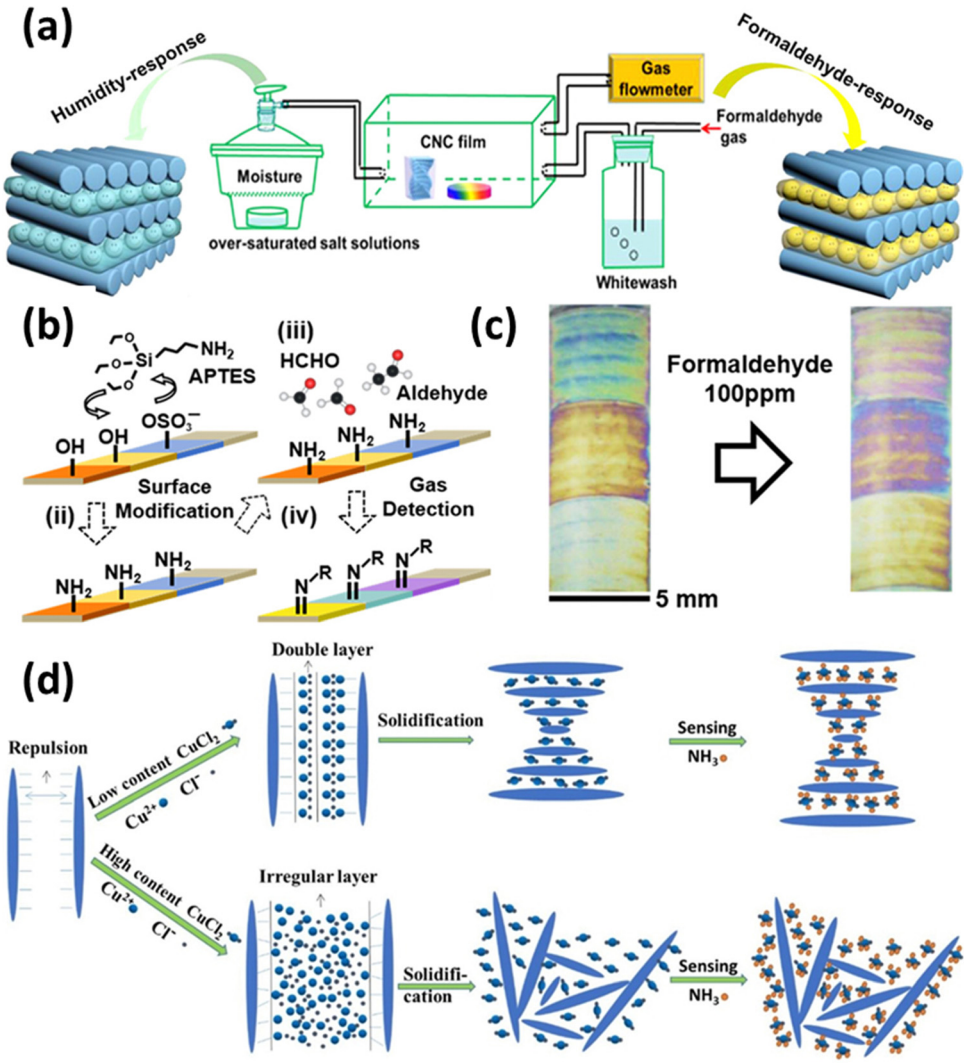

Fig. 6 Use of CNCs in gas sensing: (a) EISA assisted formaldehyde gas and humidity sensing CNCs films,[174] (b) surface alteration of CNCs and their sensing mechanism for formaldehyde gas,[175] (c) colorimetric response of prepared CNCs based probes for formaldehyde sensing,[175] and (d) CNCs based sensors for ammonia sensing and their preparation method.[149] Reproduced from ref. 174 with permission from ACS, copyright 2020. Reproduced from ref. 175 with permission from ACS, copyright 2018. Reproduced from ref. 149 with permission from Elsevier, copyright 2017.

In a study conducted by Dai *et al.*,[149] a simple, sensitive, inexpensive, colorimetric ammonia gas sensor based on a copper salt-loaded cholesteric CNCs film was developed. Copper ions can be used to fine-tune or modulate the coloration and morphology of the composite films, which is a distinguishing characteristic of the colorimetric film sensor. Due to the strong chelation affinity of copper ions to ammonia gas, composite films containing 125 mmol g^{-1} of copper ions have a high ammonia gas sensing capacity; for example, CNCs–Cu(II)125 responded positively to ammonia gas by exhibiting a total redshift of 56.34 nm. In addition, the unique conformation of the cholesteric structure of CNCs and the superb sensitivity trigger of copper ions played crucial roles in efficient colorimetric sensing (redshift). Fig. 6(d) establishes the colorimetric response of the prepared ammonia gas sensor.

In addition to contributing to photochemical smog and acid rain, nitrogen dioxide (NO_2) gas seriously harms the human respiratory system at concentrations of more than 1 ppm. Iron oxide-coated CNCs sheets were used to create an elastic and reversible responsive NO_2 gas sensor, as demonstrated by Sadasivuni *et al.*[19] The sensor offers a high sensitivity because CNCs provide the NO_2 molecules great accessibility to the sensor surface. Additionally, CNCs endow the sensor with exceptional recoverability. Additionally, CNCs have the ability to mediate and stimulate the development of an unbroken linked route among iron oxide particles, hence boosting the electrical permeation sites and producing a stronger reaction than controlling neat iron oxides.

This section infers that CNCs have vast properties like tunable surface hydroxyl groups, large surface area, H-bonding, and chiral

Open Access Article. Published on 08 Febwaliyo 2024. Downloaded on 12/09/2024 22:53:41.
This article is licensed under a Creative Commons Attribution-NonCommercial 3.0 Unported Licence.

Table 3 NC-based biosensor probes for gas sensing

Sr. no.	CNCs nanocomposites	Sensing methods	Gases detected	Detection limits	Ref.
1	PCNCs/(AgNPs)/(MoO_3NPs)	Color change	H_2S	14 ppm	176
2	CNCs-templated tin dioxide		Carbon monoxide (CO)	5–90 ppm	152
3	CNCs sheets with iron oxide		Nitrogen dioxide (NO_2)	2–200 ppm	177
4	LBL deposited CNCs	Color variation	HAc		178
5	CNCs–Cu(II)	Colorimetric transition	Ammonia gas		149
6	Chiral nematic CNCs film	Colorimetric system	Formaldehyde gas		174
7	MXene@Pd CNCs		Hydrogen (H_2)	(23.0 ± 4.0)%@4% H_2	179
8	(GO@CNCs) nanoparticles (NPs)		Acetone	5 ppm	160

nematic structure. The major identification method used for gas sensing was optical changes in the sensor, which was fabricated using CNCs and established the behavioural changes when exposed to the gases. Table 3 summarizes some important gas-sensing findings. Owing to these properties, CNCs can change their color or sense many hazardous gases or volatile chemicals. Hence, there is a lot of scope for CNCs to act as gas sensors.

4.3. Recent advances in CNCs-based sensors for chemical sensing

Chemical sensing is a technique that may be used to detect the presence of chemical compounds. In the process of chemical sensing, analytical instruments with sensitive components that undergo chemical changes in response to interactions with chemical substances and a transducer that converts the chemical changes into detectable physical signals are used.[180] CNCs films have been extensively exploited as stimulus-responsive photonic materials for chemical and physical sensing because their chiral nematic structure is susceptible to being adjusted by environmental stimuli, leading to a reversible change in structural color.[181] Various methods such as ultrasonication, magnetic-/electric-field manipulation, vacuum-assisted self-assembly, and use of additives and electrolytes may tune the helical pitch of the chiral nematic phase to change the CNCs' reflected wavelength. Water-soluble compounds are often used as the second step to co-assemble with CNCs to make structural colors evident. The blends/composites may detect chemicals, solvents, environmental stimuli, volatile organic gases, *etc.*[182] So, the upcoming sub-sections discuss the applicability of CNCs as sensors in different types of chemical compounds. Fig. 7 demonstrates the potential of CNCs in chemical sensing. Fig. 7(a) shows how the CNCs-based sensing probes can be used for distinguishing the alcohol isomers.[183] Fig. 7(b) depicts how researchers used CNCs-based sensors for identifying acetone, ethanol, ammonia, nitrous oxide, and hydrogen.[184] In a similar manner, CNCs-based materials have been used in the SAW sensors for HCl gas detection as shown in Fig. 7(c).[185]

4.3.1. CNCs-based alcohol sensors. CNCs can be used to sense alcohol, as in a study reported by Hu *et al.*,[186] CNCs and a water-soluble β-cyclodextrin polymer (PCD) are used to produce a biomass-derived chiral nematic hybrid film. The free standing iridescent CNCs–PCD film distinguishes methanol and ethanol by red, yellow, and green structural colors, allowing naked-eye

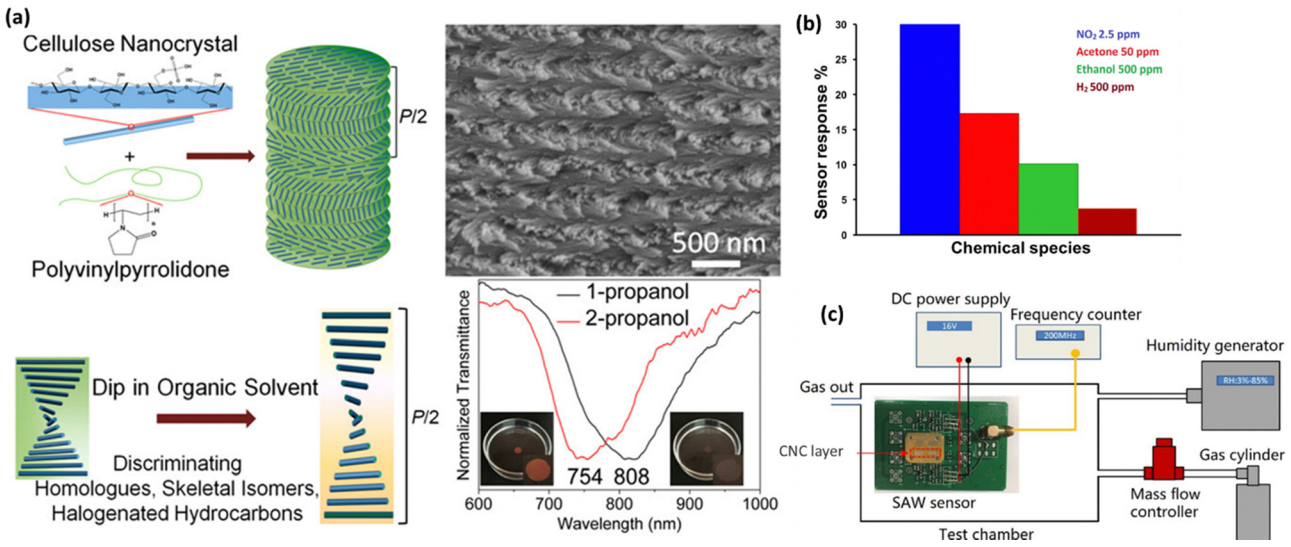

Fig. 7 Use of CNCs in physical sensing: (a) the sensing mechanism of CNCs loaded polyvinylpyrrolidone for distinguishing propanol isomers,[183] (b) a CNCs based sensor for identifying acetone, ethanol, ammonia, nitrous oxide and hydrogen,[184] and (c) similarly, a CNCs based material has been used in the SAW sensor for HCl gas detection.[185] Reproduced from ref. 183 with permission from ACS, copyright 2018. Reproduced from ref. 184 with permission from Elsevier, copyright 2019. Reproduced from ref. 185 with permission from Elsevier, copyright 2020.

© 2024 The Author(s). Published by the Royal Society of Chemistry

Open Access Article. Published on 08 Febwaliyo 2024. Downloaded on 12/09/2024 22:53:41.
This article is licensed under a Creative Commons Attribution-NonCommercial 3.0 Unported Licence.

detection. The photonic CNCs films demonstrated a clear red shift in the reflection peak with the addition of PCD. As the PCD concentration rose, the maximum reflection wavelength, which was quantified by UV-vis spectroscopy, rose from 312 to 725 nm. CNCs–PCD in other solvents maintained its same color. It altered from cyan to yellow-green for ethanol and orange-red for methanol, respectively. In addition to this, the CNCs–PCD film detects methanol in single and mixed solvents because its structural color and maximum reflection wavelength redshift most for methanol. In general, CNCs–PCD films have the potential to be used as a photonic colorimetric sensor for the quick, easy, and precise detection of methanol in industrial goods like anti-freeze and gasoline for alternative energy vehicles.

Bai *et al.*[182] produced stretchable photonic films with CNCs co-assembly using citric acid for diverse environmental stimulus responses. By adjusting the quantity of citric acid, the hydrogen-bonding interactions and electrostatic repulsion that result in such film's nematic structure and iridescent color can be altered. The plasticizing action of citric acid gives CNCs elasticity and makes the films elastic. The films may react to a variety of environmental inputs as a possible colorimetric sensor, particularly quantitatively measuring the pressure, pyridine, and compression by exhibiting apparent color changes that are visible to the human eye. We are motivated to look at the performance of the ethanol response in both the gas and liquid states because of the structural color change. The CNCs–citric acid film exhibits a red-shifted color change with an increase in the extinction wavelength from 560 to 684 nm after being immersed in anhydrous ethanol for 30 s. In particular, multifunctional photonic CNCs can be used to create anti-counterfeiting inks that make patterns and codes that can only be seen under specific lighting conditions, decorative coatings that exhibit changed colors in response to environments, and colorimetric sensors for the precise detection of alcohols.

Khan and colleagues[134] have discovered a new variety of chiral mesoporous photonic resin identified through the utilisation of cellulose nanocrystals as a template in conjunction with phenol-formaldehyde (PF) resin (Fig. 8(a)). The material's scalability and simplicity of synthesis, in addition to its photonic properties resulting from its chiral nematic structure, flexibility, and mesoporosity, render it highly appealing for utilisation in sensing, optics, and security functions. As shown in Fig. 8(b), the CNC composite films seem bright red when seen through a left-handed circular polarizer and become dull brown when viewed *via* a right-handed circular polarizer. The fabricated composites demonstrated the capability to detect solvents in an ethanol–water mixture. The composite

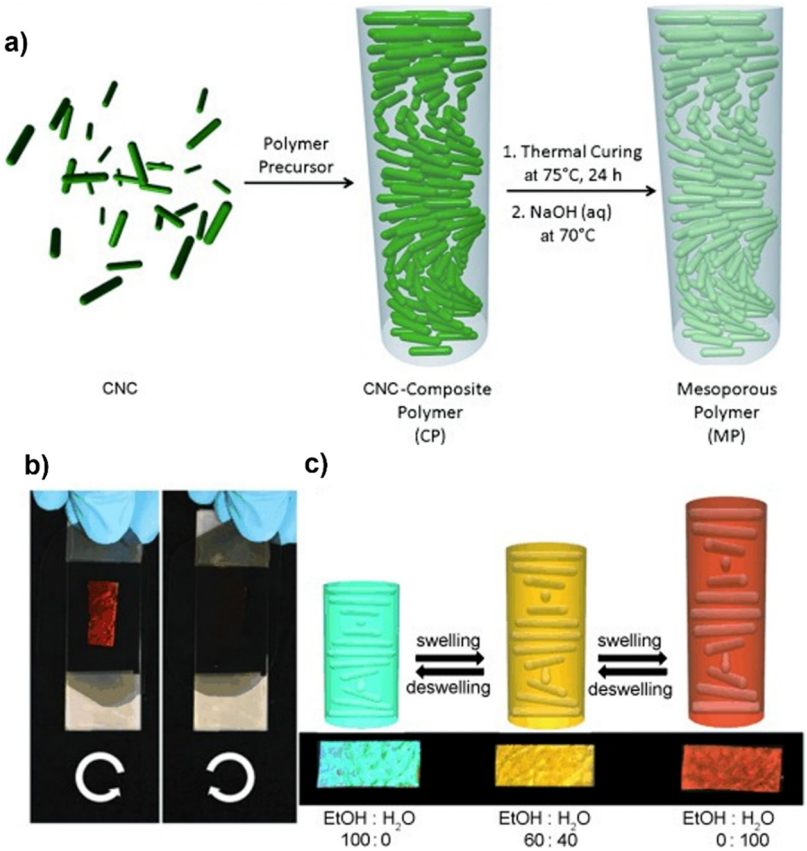

Fig. 8 (a) Mesoporous chiral nematic PF resin synthesis, (b) the manufactured film's brilliant red appearance under a left-handed circular polarizer and its disappearance under a right-handed polarizer, (c) and the optical behaviour of the CNCs-composite films in different water and ethanol mixtures.[134] Reproduced from ref. 134 with permission from John Wiley and Sons, copyright 2013.

Open Access Article. Published on 08 Febwaliyo 2024. Downloaded on 12/09/2024 22:53:41.
This article is licensed under a Creative Commons Attribution-NonCommercial 3.0 Unported Licence.

underwent a color change subsequent to the verification of the ratio of water and ethanol (Fig. 8(c)). Similar studies were reported by changing the PF to urea formaldehyde (UF) followed by polymerisation and the prepared composite had the capability to show response towards the ethanol–water mixture.[187]

Gao *et al.*,[183] in their research, created flexible nanocomposite films using CNCs that were chiral-nematically organized and amorphous polyvinylpyrrolidone (PVP). The PVP offered three significant aspects as an additive in the CNCs self-assembled architecture. The first is that PVP cannot be cross-linked since it is a neutral, amorphous polymer. Therefore, even in composites with up to 70% PVP content, its addition has no impact on the CNCs self-assembled nanostructure. The second is that PVP's solubility increases the versatility of CNCs-based composite films in various organic solvents. The third is that for CNCs/PVP composites dipped in comparable organic solvents, raising the PVP content would increase the color difference of those composites. The emphasis is on the iridescent color shift of CNCs/PVP nanocomposite films from the visible to the near-infrared region (from colored to pale) while being submerged in organic solvents for ease of recognition by the unaided eye as shown in Fig. 7(a). These CNCs/PVP nanocomposite films have demonstrated distinguishable color responses when exposed to comparable chemical solvents upon soaking, such as halogenated hydrocarbons (chloroform/dichloromethane (DCM)), skeletal isomers (1-propanol/2-propanol), and homologs (methanol/ethanol). This is due to their responsiveness to multiple solvents selectively. Additionally, CNCs/PVP composite films are effective for dipping water detection of ethanol. The CNCs/PVP system's structural color change satisfies the need for sensitive sensors. Developing sensors for various organic solvents is made easy, affordable, and effective by using CNCs/PVP composites containing chiral nematic nanostructures.

In conclusion, due to the chiral nematic structure and H-bonding, CNCs with some additives can tune these properties and can be used to form sensing films. These films will be able to sense organic compounds like alcohol by changing their color.

4.3.2. CNCs-based acid sensors. In order to sense different acids, Tang *et al.*[185] created the sensitive layer by directly hydrolyzing cotton fiber to produce CNCs, which were then spin-coated on quartz surface acoustic wave resonators. The hydroxyl groups on the surface of the CNCs can serve as absorbing sites for absorbing H_2O by creating H-bonds so that the CNCs remain partially immersed with water molecules in their ambient environment. Due to HCl's superior solubility in H_2O, adsorbable H_2O molecules may readily absorb HCl from the ambient environment. The bulk of the CNCs layer increases due to the absorption of HCl, resulting in negative responses from the SAW sensors shown in Fig. 7(c). The responses of the SAW sensor are found to be significantly influenced by ambient humidity and the thickness of the CNCs layer. With an 80 nm thick CNCs layer, the sensor responds to 1 and 5 ppm HCl gases at −2 and 10 kHz, respectively. This report concludes that CNCs possess several extraordinary properties, such as an abundance of surface hydroxyl groups and a large specific surface area, that make them suitable for acid-sensing applications.

In another report, to recognize chiral amino acids, Bi *et al.*[188] developed a new electrochemical sensor based on TEMPO-oxidized CNCs (TOCNCs) and an Au electrode that has been modified with L-cystine (L-Cys). To get additional carboxyl and L-Cys for use as a bonding agent when joining TOCNCs with Au electrodes, CNCs were oxidized by TEMPO. To evaluate the enantioselectivity of the TOCENCs/L-Cys/Au electrode, examples of the Phe, Val, and Leu enantiomers are employed. According to the experimental findings, L-amino acids exhibited a more significant peak current in cyclic voltammetry (CV) and differential potential voltammetry (DPV) when TOCNCs detected amino acid enantiomers by indicating a weaker connection with L-amino acids than with D-amino acids. The modified electrode enabled the discrimination of two enantiomers as well as the detection of one enantiomer, both of which produced outstanding results. This work offers a unique, accessible strategy for studying metabolic illnesses related to amino acids in addition to new materials for chiral amino acid recognition.

By applying the pre-stretching alignment approach and chemical and physical dual cross-linking, Zheng *et al.*[189] created an anisotropic hydrogel made of chitosan and tunicate cellulose nanocrystals (TCNCs) with vibrant interference colors. The tensile strength of the chitosan/TCNCs hydrogel was increased by the stretching alignment from 0.63 MPa to 2.06 MPa, demonstrating excellent mechanical performance. In addition to strengthening the chitosan matrix, the modest concentration of TCNCs (3.30 wt% relative to chitosan) also reflected the interference colors throughout the orientation process. Chitosan nanofiber orientation produced a birefringence look with vivid interference colors that can be controlled by adding or removing TCNCs. The hydrogels were sensitive to acidic solutions; they expanded quickly, causing a significant volume shift and the disappearance of the interference color (equilibrium is reached in approximately 2 minutes in the pH = 3 solution). It is possible to quantitatively quantify or visually witness the unique interference color variations of the oriented chitosan/TCNCs hydrogels under various pH conditions. These acid responsive anisotropic chitosan/TCNCs hydrogel demonstrated their potential for use as sensors and environmental monitors.

4.3.3. CNCs-based miscellaneous chemical sensors. Other chemicals, including propane, ethyl ether, toluene, and benzene, have caused significant environmental and public safety problems. The constant development of effective sensors that take advantage of changes in the electrochemical, optical, chromic, and conducting characteristics of sensor matrices is necessary to meet the rising need for the detection of chemicals. Using bacterial nanocellulose (BC) as a substrate, Núñez-Carmona *et al.*[184] developed biocompatible BC/ZnO gas sensors. The traditional alumina substrates used for the deposition of sensing layers are energy-intensive and not ecologically friendly since they need a lot of energy. The resulting sensors

© 2024 The Author(s). Published by the Royal Society of Chemistry

Open Access Article. Published on 08 Febwaliyo 2024. Downloaded on 12/09/2024 22:53:41.
This article is licensed under a Creative Commons Attribution-NonCommercial 3.0 Unported Licence.

respond well to ethanol, acetone, and nitrogen dioxide, as depicted in Fig. 7(b).

Similarly, CNCs can also be used to detect organic dyes such as malachite green (MG); Ogundare *et al.*[190] developed a nanocomposite sensor based on silver nanoparticles, silica, and CNCs (AgNPs/SiO_2/CNCs). CNCs serve as both a reducing and stabilizing agent in the manufacture of AgNPs. Sol–gel was used to prepare the silica, and the additional CNCs stopped AgNPs from aggregation. The resulting AgNPs, SiO_2, and CNCs nanocomposite worked well as a substrate for the fungicide and pesticide's surface-enhanced Raman scattering.

A successful approach was demonstrated by Hiratani *et al.*[191] to stabilise a hydrogel network containing large mono-domain CNCs in an isotropic state, devoid of any disorder, in purified water, by capturing the nematic organisation of these CNCs within the network *via* the shearing process as shown in Fig. 9(a). While maintaining their mono-domain structure, sheared CNCs hydrogels exhibit anisotropic swelling/shrinking characteristics that are dependent on salt concentration (ionic strength); this enables the observation of a switch in transmission colour between crossed polarizers, which is caused by a modification in the birefringence resulting from a variation in the density of CNCs. Fig. 9(b) and (c) shows the swelling and shrinking behavior of CNCs in ionic liquid and different colors with varying concentrations of NaCl solution viewed under crossed polarizers whose polarisation axis is fixed at 45° with respect to the shear direction. Furthermore, the birefringence of the hydrogels remains essentially unchanged as they undergo a colour change in response to pressure applied, which is primarily caused by a variation in sample thickness (Fig. 9(d)). Using the birefringence of CNCs-reinforced hydrogels, these outcomes illustrate a novel method of detection.

Wang *et al.*[192] reported the fabrication of a transparent and flexible cellulose/KOH-based composite ionic film (CKF) as a humidity sensor. Achieving a high optical transmittance (87.14% at 550 nm) with CKF is an uncommon occurrence among humidity sensors. This is due to the dense packing and uniform distribution of amorphous KOH induced by water evaporation and the resulting small pore size of the cellulose matrix, which is achieved by soaking and dehydrating the material. Additionally, CKF exhibits resilient mechanical properties and flexibility. In the range of 11.3% to 97.3% relative humidity (RH), the conductive CKF exhibits a reversible and rapid response in real-time to the change in RH. Its conductance fluctuates more than two hundred times and its response and recovery times of 6.0/10.8 s are considerably shorter than the majority of previously reported values. Furthermore, its hysteresis error of 0.57% is considerably lower than that documented in the literature.

Based on the information presented in this section, it can be inferred that CNCs have presented significant prospects for advancements in the field of chemical sensing, with their composites exhibiting considerable promise for further investigation in chemical sensing detection. Additionally, it has been observed that both optical and fluorimetric changes occurred

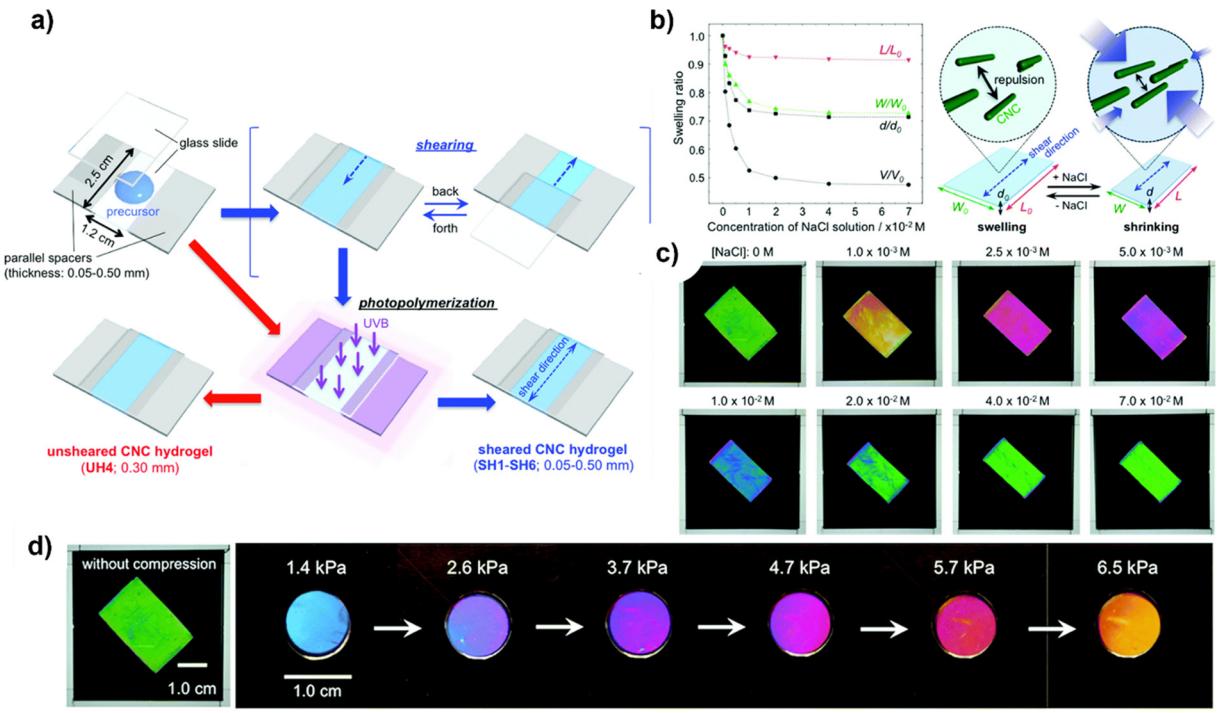

Fig. 9 (a) Sheared/unsheared CNCs hydrogel preparation; (b) ionic strength-induced swelling behaviour and change in optical properties of the sheared CNCs hydrogel with varying concentrations of NaCl solution and illustration to explain the anisotropic swelling behaviour; (c) spectra of CNCs with varying concentrations of NaCl solution viewed under crossed polarizers whose polarisation axis is fixed at 45° with respect to the shear direction; and (d) transmission images under crossed polarizers with varying pressures.[191] Reproduced from ref. 191 with permission from RSC, copyright 2018.

Open Access Article. Published on 08 Febwaliyo 2024. Downloaded on 12/09/2024 22:53:41.
This article is licensed under a Creative Commons Attribution-NonCommercial 3.0 Unported Licence.

Table 4 NCss-based biosensor probes for chemical sensing

Sr. no.	CNCs nanocomposites	Sensing methods	Chemicals detected	Detection limits	Ref.
1	(1-Butyl-3-methylimidazolium)	Colorimetric	Formaldehyde or propanal		175
2	CNCs–BPP2VA composite films	Fluorescence	HCl vapors	$1–10^3$ ppm	193
3	(NHPC) by carbonizing CNCs and urea		Ascorbic acid (AA)	2.45×10^{-7} M	194
4	Fe3O4@CNCs/Cu/GSPE	Fe_3O_4 and CuNPs	Venlafaxine	0.05–600.00 μmol L^{-1}/ 0.01 μmol L^{-1}	195
5	Cellulose nanocrystal/graphene oxide	Relative capacitance	Humidity		196
6	CNCs-based gold nanoclusters	''ON or OFF'' of fluorescence	Carcinoembryonic antigen biomarker	0.54 ng mL^{-1}	197
7	CNCs–PCD film	Colorimetric sensor	Methanol		197
8	CNCs and polyvinylpyrrolidone (PVP)	Colorimetric sensor	Homologues (methanol/ethanol), skeletal isomers (1-propanol/2-propanol)		183
9	Isothiocyanate and rhodamine B acceptors using CNCs		Intracellular pH	pH of 5.0–7.4	198
10	CNCs–rGO/SPE		MP	0.2–0.9 mmol L^{-1}/ 0.1 mmol L^{-1}	199
11	PEDOT/AuNPs/C-NCC/GCE		Vitamin C	0.88 μM to 15 000 μM	200
12	CNCs and citric acid (CA)	Color changes	Ethanol and alkali		182

when the sensors based on CNCs were subjected to the stimuli. Table 4 describes the details of the chemical sensing-based sensors and findings.

4.4. Recent advances in CNCs-based sensors for physical stimuli sensing

The fourth most common types of sensors made from nanocellulose composite materials are those that respond to physical inputs. This type of sensor examines changes in electricity that are caused by physical changes. This type of sensor can be classified into four types: piezo, heat, electric, and pH-sensitive. To make an intelligent physical stimuli-responsive probe that can be used in many different situations, it needs to be able to stretch highly, be flexible, be more sensitive, and have a more comprehensive sensing range towards change in physical environments. Fig. 10 shows the use of CNCs in physical sensing, Fig. 10(a) shows PU/tCNCs based wearable sensors and their working mechanism,[201] Fig. 10(b) shows CNCs/PNIPAM based multi-responsive hydrogels,[202] Fig. 10(c) depicts CNCs based 3D printed pyro-piezoelectric sensors for human machine interface monitoring,[203] and Fig. 10(d) demonstrates pH sensitive PVA/CNCs films for visual shrimp freshness monitoring.[204]

4.4.1. CNCs-based piezo sensors. The term ''piezo'' originates from the Greek language, specifically meaning ''press'' or ''squeeze.'' Consequently, a piezoelectric sensor operates by quantifying compression through the use of the piezoelectric effect. The piezoelectric sensor can transform various physical factors, such as acceleration, strain, or pressure, into an electrical charge that may afterward be quantified. These entities possess high sensitivity and exhibit diminutive dimensions, rendering them particularly suitable for integration into everyday products.

In their study, Li *et al.*[205] developed lightweight and portable self-powered piezoelectric sensors using CNCs as porous materials. However, they observed that unmodified CNCs did not exhibit sufficient piezoelectric properties without intense external polarization. This was attributed to the irreversible deformation caused by their low toughness. They successfully bonded rod-like CNCs with a flexible polymer, specifically polyethylene glycol (PEG). Their hypothesis was that incorporating PEG would enhance the material's mechanical strength while enabling the CNCs to exhibit polarisation in response to the dielectric signal. They employed the technique of adsorbing graphene (GR) onto the surface electrodes to fabricate a piezoelectric porous material known as CNCs–PEG–GR. The resulting material exhibited a density of 0.096 g cm^{-3}. The voltage output attained its peak value when the frequency aligned with the dielectric relaxation frequency of PEG. Additionally, the length-to-diameter ratio of the pores in the porous material was enhanced from 1.1 to 3.3 through modifications made to the freeze-drying process. As a result, the voltage output was able to reach 0.7 V at a moderate ratio. Such portable self-powered sensors have a great scope and can be readily integrated into intelligent wearable electronic gadgets.

Stretchable chiral nematic cellulose nanocrystals (CNCs)–elastomer composites that display reversible visible coloration in response to mechanical stress were reported by Boott *et al.*[206] The colour of the CNCs–elastomer composite undergoes a transition from red to green to blue as it is elongated. This transition occurs as a result of mechanical tension compressing the helical pitch of the chiral nematic organisation. The development of reversible visible colour chiral nematic CNCs–E represents a substantial advancement in the fabrication process of responsive photonic crystals.

A flexible pressure sensor was developed by Chen *et al.*[207] utilising a nanocellulose composite aerogel and a straightforward fabrication method. The sensor exhibited adjustable sensitivity over a broad pressure range of 0–100 kPa. Using directional ice-templating and freeze-drying, composite aerogels with modifiable porous structures were produced utilising carbonised bacterial nanocellulose, which possesses

 © 2024 The Author(s). Published by the Royal Society of Chemistry

Open Access Article. Published on 08 Febwaliyo 2024. Downloaded on 12/09/2024 22:53:41.
This article is licensed under a Creative Commons Attribution-NonCommercial 3.0 Unported Licence.

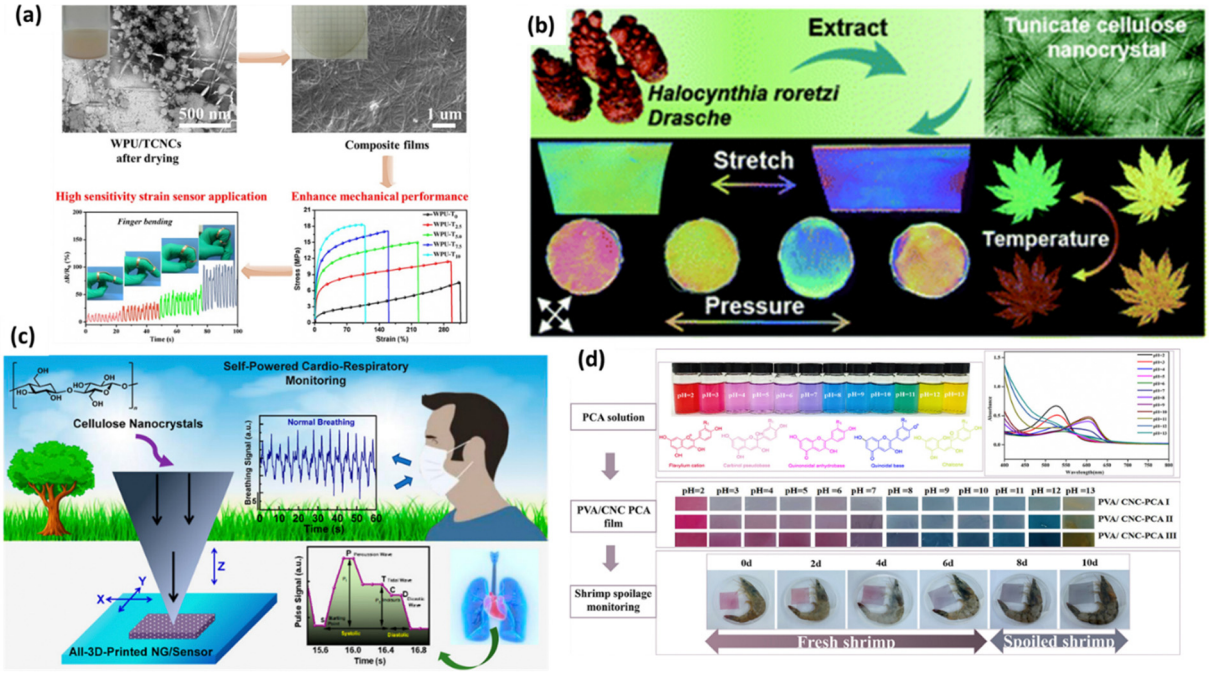

Fig. 10 Use of CNCs in physical sensing: (a) PU/tCNCs based wearable sensors and their working mechanism,[201] (b) CNCs/PNIPAM based multi-responsive hydrogels,[202] (c) CNCs based 3D printed pyro-piezoelectric sensors for human–machine interface monitoring[203] and (d) pH-sensitive PVA/CNCs films for visual shrimp freshness monitoring.[204] Reproduced from ref. 201 with permission from Elsevier, copyright 2023. Reproduced from ref. 202 with permission from RSC, 2021. Reproduced from ref. 203 with permission from ACS, copyright 2023. Reproduced from ref. 204 with permission from Elsevier, copyright 2023.

exceptional conductivity, and wood-derived CNFs. By utilising these composite aerogels as piezoresistive materials, exceptionally adaptable sensitivity, rapid response, and dependability were exhibited by the pressure sensors that were fabricated.

Miao *et al.*[85] conducted a comprehensive investigation of the piezoelectric charge response of CNCs films. The objective was to assess the impact of surface chemistry, particle morphology, ionic strength, and film microstructure on the modulation of bulk CNCs performance. The methodology employed in their study involved a scalable approach from the bottom up, resulting in the production of CNCs films. These films exhibited a consistent piezoelectric response, namely a $|d_{33}|$ value of approximately 29 pC N^{-1}, even after undergoing 440 compressive cycles. The piezoelectric response of CNCs–polyethylene oxide nanocomposites, which were both flexible and transparent, was found to be comparable, with a value of $|d_{33}|$ of about 23 pC N^{-1}. These prepared materials present noteworthy technological prospects for the utilization of renewable CNCs in the development of flexible organic field-effect transistors and multifunctional sensors.

Cao *et al.*[208] have identified an unprecedented hierarchical structure within a novel photonic aerogel that is responsive to pressure. By means of ice templating, CNCs self-assemble into chiral nematic filaments within a three-dimensional macroporous network. Upon compression in a polar solvent, the aerogel undergoes a transition from a three-dimensional cellular structure to a two-dimensional planar configuration, resulting in a modification of its optical characteristics from broadband dispersion to Bragg diffraction. Shape recovery composites were produced by infiltrating a 3D aerogel with PDMS; these composites exhibit structural coloration when subjected to pressure but revert back to white upon release. The development of a solvent-responsive ink was additionally motivated by this novel mechanoresponsive mechanism; this ink facilitates the writing process on a wide range of substrates and reacts rapidly with various solvents.

Maity and his colleagues[203] reported an all-three-dimensional (3D)-printed pyro-piezoelectric nanogenerator (Py-PNG) made of CNCs, which are the most common and utterly biodegradable biopolymers on earth. They proposed a new way to create an NG sensor using 3D geometry. It was printed in a unique way using only 3D printers, and it has the potential to reduce the number of processing steps and pieces of equipment needed during multilayer fabrication. The NG sensor was made out of only 3D-printed parts with great mechano-thermal energy harvesting performance and sensitivity, and it can accurately identify the heartbeat and breathing whenever and however it is needed, without a battery or an external power source. They also showed an intelligent mask-based breath-tracking system that can be used with this technology. So, real-time cardiorespiratory tracking gives essential and interesting information for medical diagnosis, which is a step towards biomedical device development and human–machine interfacing.

Kose *et al.*[209] introduced an elastomeric nanocomposite material that is both homogeneous and highly stretchable,

Open Access Article. Published on 08 Febwaliyo 2024. Downloaded on 12/09/2024 22:53:41.
This article is licensed under a Creative Commons Attribution-NonCommercial 3.0 Unported Licence.

and it incorporates chiral nematic structures of CNCs. When the external stress is removed, the exceedingly flexible composite returns to its initial shape after undergoing an elongation of more than 900% (elongation without hysteresis is observed within 300%). The chiral nematic organization of the CNCs is remarkably unwound by stretching the polymer, resulting in nanocrystal alignment within the elastomer and, as a consequence, robust birefringence. The stretched composite exhibits vibrant interference colors as a result of an optical axis that becomes apparent in the direction of elongation. The intriguing un-winding of the Bouligand structure presents a promising avenue for the development of reversible stimuli-responsive materials, which could find utility in fields such as flexible optics and sensing.

In a study reported by Deng *et al.*,[201] TCNCs were mixed with castor oil-based waterborne polyurethane (WPU) using a straightforward solution blending technique to create bio-based nanocomposites. The impact of TCNCs on the particle size and stability of composite dispersions and the thermo-physical and mechanical properties of composite films was investigated and discussed. Not only did the unique structure and properties of TCNCs, such as high crystallinity, large aspect ratio, and high modulus, significantly improve the storage stability of WPU, but they also demonstrated significant reinforcing/toughening effects and outstanding compatibility with WPU. By drip-coating silver nanowires (AgNWs) on the surface of the composite films, flexible strain sensors were fabricated that demonstrated exceptional sensitivity in monitoring human movement.

Zheng *et al.*[210] developed a new interpenetrating polymer network (IPN)-structured hydrogel utilizing chemically cross-linked poly(acrylic acid) and physically cross-linked poly(vinyl alcohol) to impart stretchability, toughness, and conductivity (Fig. 11(a)). Upon the incorporation of CNCs chains, the tensile strength and resilience were considerably improved. Furthermore, the hydrogel-based sensor that was developed demonstrated the ability to precisely distinguish between minor and major bodily movements, including finger bending, limb rotation, and pulse as shown in Fig. 11(b).

In their study, Kose *et al.*[211] presented shear-aligned pseudonematic CNCs that are embedded within a homogeneous poly(ethyl acrylate) elastomer. Fig. 11(c) shows the schematic for the formation of a CNCs based elastomer. This composite material demonstrates reversible optical properties when subjected to mechanical stimuli. When observed through crossed or parallel polarizers, the relaxed composite exhibits a vibrant interference colour due to the long-range anisotropy of CNCs. Stretching the pseudonematic CNCs elastomer in a direction parallel to the CNCs alignment results in enhanced CNCs alignment and an increase in the birefringence of the materials. When the composite is stretched perpendicular to the direction of CNCs alignment, however, the CNCs become more

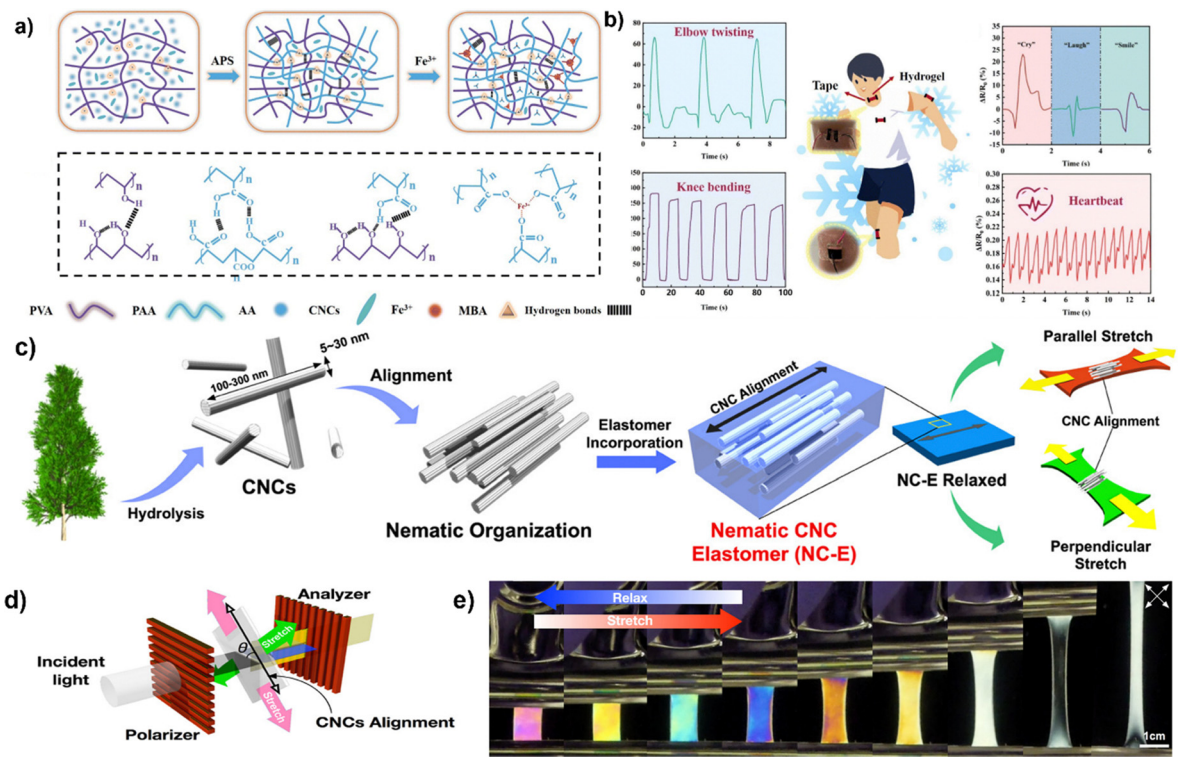

Fig. 11 (a) Schematic representation of hydrogel formation,[210] (b) the resistance variation curves of the hydrogel strain sensor, which is based on CNCs, are shown schematically for different movements: elbow twisting, knee bending, speaking, and heartbeat,[210] (c) illustration of the procedure for creating the CNCs elastomer with unidirectional alignment,[211] (d) schematic diagram demonstrating the use of polarised light to examine elongated samples,[211] and (e) the interference colours are detected when the sample is stretched in a direction perpendicular to the alignment of the CNCs.[211] Reproduced from ref. 210 with permission from RSC, 2022. Reproduced from ref. 211 with permission from ACS, copyright 2019.

© 2024 The Author(s). Published by the Royal Society of Chemistry

Open Access Article. Published on 08 Febwaliyo 2024. Downloaded on 12/09/2024 22:53:41.
This article is licensed under a Creative Commons Attribution-NonCommercial 3.0 Unported Licence.

disorganised and the birefringence falls. This led to variations in the optical response to distinct mechanical stimuli and the restoration of the initial colour when the subject relaxed as depicted in Fig. 11(d) and (e). Overall with these key findings CNCs can be a potential candidate for sensing applications.

4.4.2. CNCs-based heat sensors. A temperature sensor is a tool utilized for the purpose of detecting changes in temperature. The temperature being referred to can comprise air temperature, liquid temperature, or the temperature of a solid substance. In recent years, there has been a significant focus on temperature sensor fabrication due to the emergence of flexible substrates based on nanocellulose. Flexible substrates are predominantly utilized in a range of applications related to temperature sensing.

The fabrication of mechano-thermo-chromic hydrogels with consistent interference colors was reported by Wang *et al.*[202] This was achieved through the directional shearing of CNCs and subsequent immobilization of these aligned CNCs within poly(*N*-isopropylacrylamide) (PNIPAM) networks. The manifestation of iridescent birefringence was observed at a reduced concentration level due to the increased aspect ratio and crystallinity of the CNCs. The chromatic shift observed in the POM photos exhibited a strong correlation with the temperature, confirming the OH sample's reversible and thermo-responsive nature. The extensive range of stimuli to which OH exhibits a responsive behavior and its high degree of repeatability render it advantageous for employing OH as a visual temperature sensor in real-world scenarios. Their study presents a novel approach for the development of sustainable and flexible responsive optical devices utilizing such CNCs. These devices have potential applications in various fields, such as sensing technology, environmental monitoring, and anti-counterfeiting measures.

The successful preparation of CNCs-based thermo-responsive fluorescent composites was reported by Chen *et al.*[212] They utilized metal-free surface-initiated atom transfer radical polymerization (ATRP) of NIPAAm and a Schiff base-containing dye (HDPAP). The findings of the study indicate that composites of CNCs–poly(NIPAAm-HDPAP) exhibit a temperature-responsive coil-to-globule transition behavior at the lower critical solution temperature. Furthermore, the utilization of light-mediated atom transfer radical polymerization (ATRP) has been demonstrated as a highly promising approach for the production of multifunctional nanomaterials. This process offers unparalleled advantages such as reduced energy consumption, enhanced efficiency, excellent compatibility with various monomers, and the absence of transition metal ions.

Xu *et al.*[213] developed an injectable thermo-sensitive hydrogel (composed of chitosan/glycerol phosphate sodium/cellulose nanocrystals, CS/GP/CNCs) that effectively contained human umbilical cord mesenchymal stem cells (hUCMSCs) for the purpose of repairing full-thickness cutaneous wounds. The incorporation of CNCs into the CS/GP system resulted in a notable enhancement in both the gelation rate and mechanical characteristics while concurrently reducing the rate of deterioration. The histological analysis revealed that the combination of hydrogel and human umbilical cord mesenchymal stem cells (hUCMSCs) had a notable impact on various aspects of wound healing. Specifically, it was seen that this combination expedited the closure of wounds, improved microcirculation, facilitated tissue remodeling, promoted re-epithelialization, and stimulated hair follicle regeneration. Additionally, it was shown that the combination treatment effectively suppressed excessive inflammation in both the core and surrounding areas of the wounds. The combination of hydrogel and human umbilical cord mesenchymal stem cells (hUCMSCs) increased collagen deposition and the expression of the mature keratinocyte marker K1. Additionally, the secretion of inflammatory factors, specifically TNF-α and IL-1β, was reduced. Their research presented a viable therapeutic approach for addressing non-healing chronic cutaneous lesions.

4.4.3. CNCs-based pH sensors. A pH sensor is one of the most significant tools for detecting pH and is typically utilized to check water quality. This particular type of sensor can determine solution's alkalinity and acidity levels, like water, for example. pH sensors, when used correctly, have the ability to ensure the quality and safety of products and processes that take place in wastewater treatment plants or manufacturing facilities. CNCs have also garnered the attention of researchers to develop pH-responsive sensors for water remediation and safer life.

The objective of the study conducted by He *et al.*[204] was to fabricate a novel film for pH sensing. This film was developed by immobilizing purple cabbage anthocyanins (PCA) within a matrix of polyvinyl alcohol (PVA), which was further reinforced using CNCs. Incorporating CNCs and PCA led to improvements in the UV-visible barrier, mechanical qualities, and moisture resistance. The incorporation of PCA resulted in the videos acquiring intelligent characteristics. The films loaded with PCA exhibited pronounced colorimetric responses to changes in pH within the range of 2 to 13 and to the presence of volatile ammonia. These responses were visually discernible. When utilized to monitor the freshness of prawns at a temperature of 4 °C, films composed of PVA/CNCs and containing 0.6% PCA demonstrated noticeable variations in color, transitioning from purple to grey-blue as the deterioration occurred. Consequently, the utilization of PVA/CNCs–PCA colorimetric films prepared by them is suitable for the purpose of intelligent package labels. These films exhibited notable mechanical strength, effective water vapor barrier characteristics, and the ability to sense pH levels, which made them well-suited for the visual assessment of the quality of fresh seafood products.

Nielsen and coworkers[214] have developed the process of converting dual fluorescent labelling cellulose nanocrystals into ratiometric pH-sensing nanoparticles *via* a straightforward one-pot reaction. In addition, a straightforward and adaptable three-step method for increasing the number of fluorophores accessible for transplantation was illustrated (Fig. 12(a)). Esterification was used to introduce an amine group, which was then followed by a thiol–ene click reaction. They were able to distinguish the response of the prepared CNCs based sensor over a pH of 5 to 8.

Open Access Article. Published on 08 Febwaliyo 2024. Downloaded on 12/09/2024 22:53:41.
This article is licensed under a Creative Commons Attribution-NonCommercial 3.0 Unported Licence.

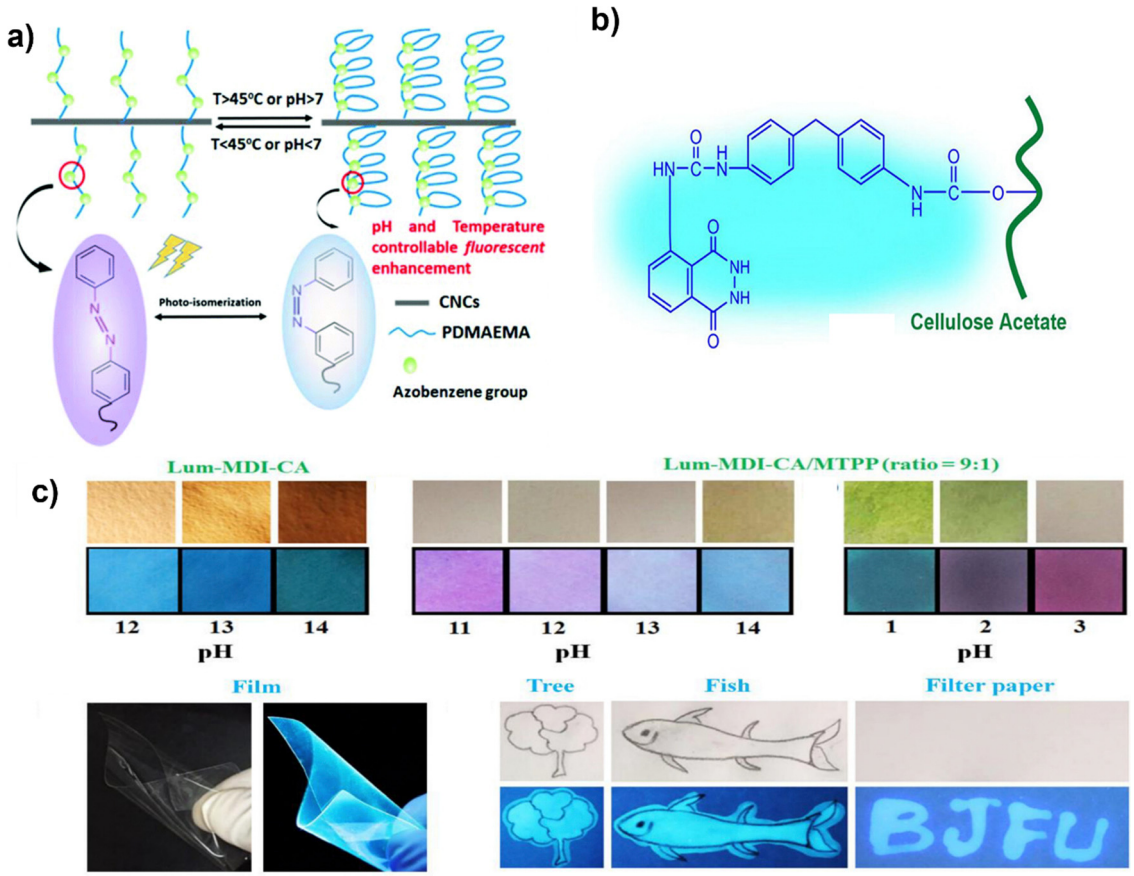

Fig. 12 (a) Schematic representation of the temperature- and pH-responsive characteristics, photo-isomerization, and fluorescence performance of CNCs-based nanosensors,[214] (b) structure of Lum–MDI–CA, and (c) the development of transparent flexible fluorescent films and pH strips that use Lum–MDI–CA solution to distinguish between very alkaline pH values.[215] Reproduced from ref. 214 with permission from RSC, 2010. Reproduced from ref. 215 with permission from ACS, copyright 2023.

Nawaz *et al.*[215] prepared a biopolymer-based structure (Lum–MDI–CA, Fig. 12(b)) by chemically bonding luminol to cellulose acetate (CA) *via* the cross-linking agent 4,4′-diphenylmethane diisocyanate (MDI), which incorporates responsive functional groups including –C═O and –NH. By altering colors within a narrow pH range under visible light and at 365 nanometers, the surface-tuned CA that was prepared distinguishes acutely acidic pH 1 from pH 2 and extreme alkaline pH 12, 13, and 14. Fig. 12(c) shows the colour change under extreme alkaline conditions and Lum–MDI–CA/DMSO solution (20 mg mL^{-1}) was made to manufacture a fluorescent ink for the creation of security patterns, such as fish, trees, and BJFU letters. A little brush was used to express the aforementioned security designs on the filter paper. In conclusion we can say that this study provides a cutting-edge method for creating bio-based smart materials with several uses.

A general and uncomplicated approach is illustrated in the research conducted by Kelly *et al.*[216] for the synthesis of novel nanocomposite hydrogels featuring photonic properties and long-range chiral nematic structure. Variations in iridescence are observed in the hydrogels when exposed to external stimuli, including solvent, pH, or temperature. In addition, the utilisation of CNCs to modify the surface of the hydrogel exhibits potential as an innovative method for customizing the material's behavior and fabricating novel substances that possess chiral optoelectronic characteristics. Redshifting enabled the prepared CNCs-based hydrogels with chiral nematic ordering to differentiate over a broad pH range of 7 to 13.

In a study conducted by Yuan *et al.*,[217] a novel fluorescent nanosensor called CNCs-*g*-P(AzoC6MA-*co*-DMAEMA) was developed through an atom transfer radical copolymerization (ATRP) reaction involving AzoC6MA and DMAEMA and cellulose nanocrystals (CNCs) modified with 2-bromoisobutyryl groups (CNCs-Br) as the initiators. The sensor constructed from CNCs demonstrated operational capability in aqueous solutions and fluorescence properties across a pH range of 4 to 10.

In their study, Khanjanzadeh *et al.*[218] produced pH-indicator films using the covalent bonding of activated bromocresol purple (a-BCP) with esterified cellulose nanocrystals (e-CNCs). These films were designed specifically for applications requiring pH-sensitive color changes. The cellulose acetate polymer was modified by adding e-CNCs/a-BCP particles to fabricate films that exhibit pH-sensitive color changes. The colorimetric investigation revealed that films with 10% or 15% e-CNCs/a-BCP particles exhibited significant alterations in color at either pH 4–5 or pH 7–8. The films containing 10% e-CNCs/a-BCP

© 2024 The Author(s). Published by the Royal Society of Chemistry

Open Access Article. Published on 08 Febwaliyo 2024. Downloaded on 12/09/2024 22:53:41.
This article is licensed under a Creative Commons Attribution-NonCommercial 3.0 Unported Licence.

particles showed remarkable resistance to leaching when exposed to acidic conditions. The observed alterations in color demonstrated reversibility within the pH range of 2 to 10. The pH-indicator films showed observable alterations in color in accordance with changes in pH levels. These films also demonstrated the ability to reverse their color changes, resist leaching, and maintain adequate stiffness. However, it should be noted that the mechanical characteristics of the films declined as the concentration of e-CNCs/a-BCP grew from 0% to 15%. Consequently, their research findings provide empirical evidence in favor of the proposed hypothesis, suggesting that cellulose acetate (CA) films incorporating e-CNCs/a-BCP particles show significant promise as pH-sensitive films within packaging applications.

The researchers, Xiao *et al.*,[219] successfully synthesized nanocapsules called spherical curcumin/polyvinylpyrrolidone nanocapsules (CurNC), which exhibited enhanced water solubility and thermal stability compared to natural curcumin (Cur). In this study, they constructed pH-sensitive multifunctional packaging films using the soy protein isolate as the primary material. These films were then reinforced with CNCs to enhance their mechanical properties. Four different variations of the films were created: CurNC, CNCs/CurNC, CNCs/Cur, and CNCs. The purpose of these films was to detect the freshness of prawns. The incorporation of agents containing CNCs was shown to enhance many properties of the film, including tensile strength, hydrogen bond interactions, thermal stability, and crystalline structure. Simultaneously, it resulted in a reduction in water solubility, as well as lower permeability to water vapor and oxygen. It is worth noting that the CNCs/CurNC film exhibited more antiradical scavenging activity compared to the CNCs/Cur film. Additionally, the CNCs/CurNC film demonstrated notable sensitivity to variations in pH and the presence of NH_3. Furthermore, the prepared CNCs/CurNC film exhibited the capability to reduce the overall volatile basic nitrogen content in preserved prawns and effectively monitor the freshness of prawns in a live and continuous manner.

This section provides an overview of the various applications of physical stimuli-responsive CNCs-based sensing probes, including health monitoring, piezoelectric, and packaging. The primary methods of detection encompassed fluorescence and optical responses to the physical stimuli. A summary of key findings regarding stimuli-responsive CNCs-based sensors is provided in Table 5. The potential for further exploration exists in more recent domains of application, such as energy storage and energy harvesting.

4.5. Recent advances in CNCs-based sensors for biomaterial sensing

Biosensors are regarded as top-notch investigative instruments with a wide range of uses, including in clinics and diagnostics for various sorts of samples. Recently, functional and intelligent biosensors that are made from renewable materials have sparked a lot of attention. Low-cost, functional substances with passive liquid transportation and biodegradability are appealing for sensing applications.[229] Despite having unique and valuable qualities, CNCs have weak electrical conductivity and are unable to provide sufficient sensitivity for biosensor applications. Additionally, CNCs are extremely hydrophilic and incompatible with specific sensing molecules, and so they must be modified in order to be employed as a suitable supporting material in biosensor applications.[230] CNCs and electronic components were combined to create multiple multifunctional devices, which were used in a variety of applications, including biosensing. Hence, the role of CNCs in different types of biosensors is discussed in the following subsections. Table 6 briefly summarizes the recent findings in the field of CNCs-based biomaterial sensors. Fig. 13 demonstrates the applicability of CNCs as biosensors. Fig. 13(a) depicts a schematic representation of CNCs based sensors for glucose,[231] Fig. 13(b) shows the preparation methodology of CNCs-based polyelectrolytes for heparin sensing,[232] and Fig. 13(c) explains the working mechanism of prepared CNCs polyelectrolytes for heparin sensing and extraction.[232]

4.5.1. CNCs-based protein sensors. As some of the most significant functional macromolecules of organic matter in daily existence, proteins play a role in gene regulation and cell metabolism and actively defend the body's immune system, resulting in a strong biological barrier and homeostasis.[240] The considerable development in many applications, including the detection and analysis of proteins in tiny amounts, is being accelerated by advancements in CNCs. The vanguard of this revolution is protein sensing focused on nanocellulose. Nanocellulose has a significant advantage in protein sensing because of its intrinsic qualities of high biocompatibility, low

Table 5 NC-based biosensor probes for physical stimuli sensing

S. no.	CNCs nanocomposites	Sensing methods	Stimuli detected	Detection limits	Ref.
1	CNCs–PANi/PVA/borax		Strain		220
2	CNCs–PPy/PMMA/PVA				221
3	C-MX/CNCs		Pressure/strain	50 Pa–10 kPa/1 Pa	222
4	PVA/CNCs–PCA	Colorimetric	pH		204
5	GO@CNCs–poly(AAm-*co*-AAc)		Strain		223
6	AuNS/PVA/CNCs		Temperature sensor		224
7	CNCs (F-A-CNCs)		pH	2.28 to 10.84 pH	225
8	CNCs–ABA		Strain		226
9	TG/CNCs/EGS	Coloration change	pH		227
10	CNCs/PNIPAM	Color change	Humidity or heat		228

Open Access Article. Published on 08 Febwaliyo 2024. Downloaded on 12/09/2024 22:53:41.
This article is licensed under a Creative Commons Attribution-NonCommercial 3.0 Unported Licence.

Table 6 NC-based biosensor probes for biomaterial sensing

S. no.	CNCs nanocomposites	Sensing methods	Biomaterials detected	Detection limits	Ref.
1	TOCNCs/GO_x/SPE		Glucose	0.004 mM	231
2	CNCs/magnetite nanoparticle hybrid sol		Glucose	5 mM	233
3	CNCs colloid conjugated with cationic polyelectrolytes		Heparin		232
4	PANi/CNCs/IL/GLU/ChOx		Cholesterol	0.48 μM	234
5	Conjugated cotton CNCs	Colorimetric change	Human neutrophil elastase (HNE)		235
6	(GOx), (HRP) and (ABTS)	Colorimetric based	Glucose	1.5–12.8 mmol L^{-1}	236
7	(CNCs–XG)	Colorimetric change	Cellulolytic enzymes		237
8	CNCs and xyloglucan	Colour changes	Enzyme	10 mg L^{-1}	238
9	(Poly(GMA-*co*-EGDMA))		Cortisol	2.0 ng mL^{-1} ± 0.4 ng mL^{-1}	239

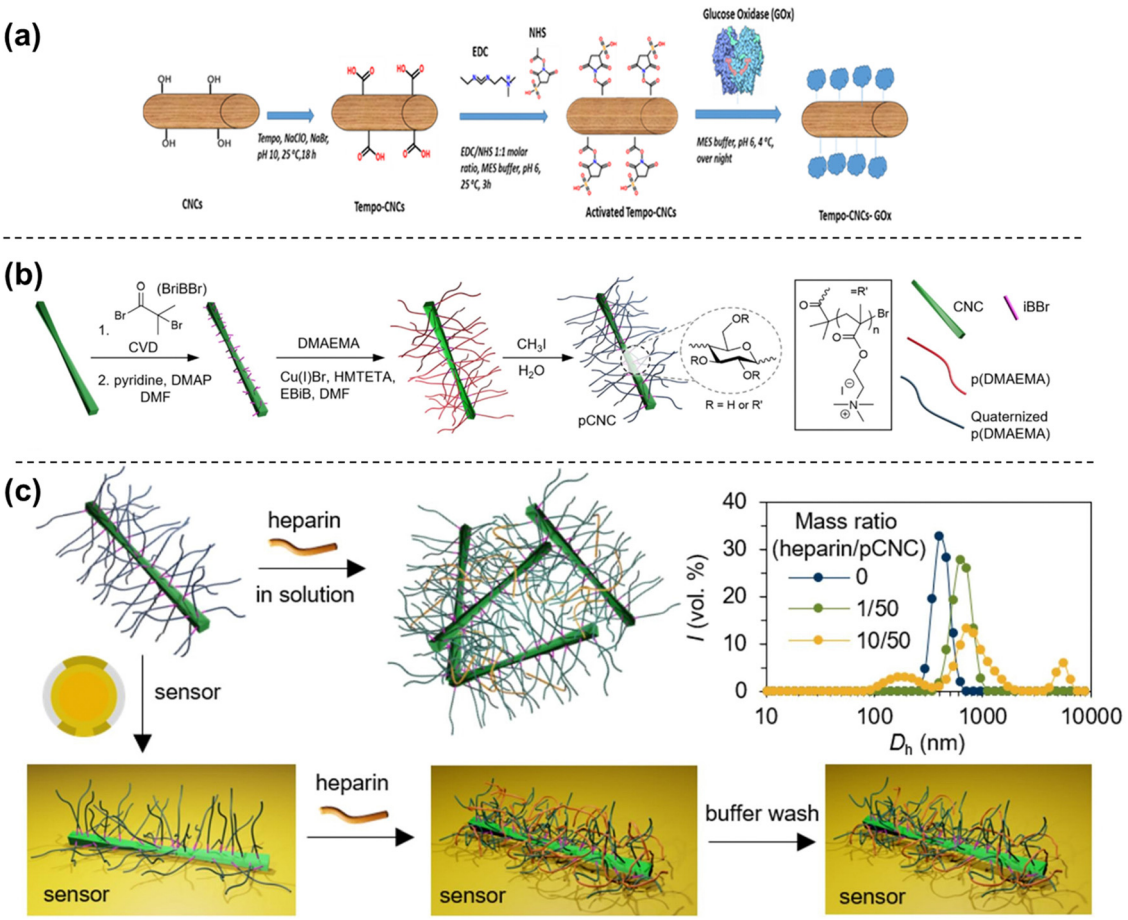

Fig. 13 Applicability of CNCs as biosensors. (a) Schematic representation of CNCs based sensors for glucose sensing,[231] (b) preparation methodology of CNC-based polyelectrolytes,[232] and (c) working mechanism of prepared CNCs polyelectrolytes for heparin sensing and extraction.[232] Reproduced from ref. 231 with permission from Biosensors, MDPI, 2020. Reproduced from ref. 232 with permission from Elsevier, copyright 2021.

cytotoxicity, high specific area, strong durability, and marketability.[241] Following are some reports on CNCs' ability to sense different kinds of proteins.

Liu *et al.*[232] used a biomass-derived CNCs colloid coupled with cationic polyelectrolytes to recover heparin. One of the most significant anticoagulant medications used in clinical settings is heparin. The methylene blue binding test and quartz crystal microbalance analysis showed that the substantial specific surface area and brush-like shape considerably boosted the heparin-capture efficiency and speed under physiologically relevant circumstances, as shown in Fig. 13(b) and (c). They also discovered that altering pH or salt content may achieve a selective heparin capture. Finally, we demonstrated that the cationic nanocrystal's ability to recover heparin was largely retained after several recycle rounds and that the majority of the active heparin dose was recovered, indicating a significantly

© 2024 The Author(s). Published by the Royal Society of Chemistry

Open Access Article. Published on 08 Febwaliyo 2024. Downloaded on 12/09/2024 22:53:41.
This article is licensed under a Creative Commons Attribution-NonCommercial 3.0 Unported Licence.

higher heparin-recovery performance than the commercial Amberlite IRA-900 and proving its viability from an economic standpoint. As a result, the newly discovered CNCs–polymer conjugate is a viable contender for effective and environmentally friendly heparin recovery.

Using quick, practical, and sensitive hydrolytic enzyme sensing techniques may considerably increase biosensor's possibility and commercial competitiveness. In order to do this, Cerclier *et al.*[238] created brand-new colored multilayered thin films employing CNCs and XG as the fundamental building block for very effective enzyme detection. The produced colored CNCs/XG thin films were easily degraded by the cellulase, which caused the color of the film to alter. Because both cellulose and the XG molecules are susceptible to cellulolytic enzymes, the sensing method over the (CN/XG)4 multilayered thin films is based on the slow destruction of the thin films by a cellulase combination. In further detail, the hydrolysis of thin films may decrease the thickness of the layer, in which the naked eye can see the enzyme's activity as a change in colour over a short period. The breakdown of the XG unit in the CNCs/XG thin film by the coexisting cellulolytic enzymes caused the film color to deteriorate when the CNCs/XG thin film was combined with cellulase. The original thickness of the CNCs/XG thin film set the first color. The fading process was visible with the unaided eye. With the ability to precisely regulate film thickness and structure, this approach not only had the benefits of being simple to use, quick, and reliable, but it could also quantitatively analyze the concentration of enzymes. This capability might be extended to the sensing of more biomass-hydrolyzing enzymes.

4.5.2. CNCs-based glucose sensors. The disease of diabetes mellitus affects people all around the globe. Blood glucose levels that are either greater or lesser than the usual range of 80–120 mg dL^{-1} (4.4–6.6 mM) indicate the presence of this metabolic condition, which is brought about by insulin insufficiency and hyperglycemia.[242] One of the leading causes of mortality and disability in the globe is illness. In order to diagnose and treat diabetes mellitus, blood glucose levels must be closely monitored.[243] That is why providing a straightforward, accurate, and affordable platform for detecting glucose is crucial, and a CNCs-based sensor is doing just that exceptionally effectively.

In a report, Dong *et al.*[244] created Au nanohybrids supported by poly(diallyldimethylammonium chloride)–cellulose nanocrystals (PDDA–CNCs) by the self-assembly of a negatively charged Au precursor and positively charged PDDA–CNCs functional groups. The Au/PDDA–CNCs nanohybrid's structural characteristics and suitability for glucose sensing were investigated. According to characterization experiments, the synthesis methodology produced well-dispersed Au nanoparticles on the PDDA–CNC support matrix with average particle sizes ranging from 3.5 to 8.4 nm based on the Au content. With a low detection limit of 2.4 μM (S/N = 3), a high sensitivity of 62.8 μA mM^{-1} cm^{-2}, and a linear detection range from 0.004 mM to 6.5 mM, the 5Au/PDDA–CNCs (*i.e.*, an Au loading level of 5 wt%) demonstrated the best glucose-sensing ability. This was attributed to the moderate size and dispersity of the Au nanoparticles. According to further research, the 5Au/PDDA–CNC nanohybrids demonstrated good selectivity and stability. These findings indicate the potential use of CNCs with metal nanoparticle decoration in electrochemical biosensing.

A screen-printed glucose sensor using TEMPO-oxidized CNCs as a biological scaffold for reliable covalent enzyme immobilization is described by Tang *et al.*[231] The TEMPO oxidizing process was used to transform the hydroxymethyl groups of CNCs into their carboxylic form, resulting in carboxylic-CNCs (TEMPO-CNCs). The carboxyl groups of TEMPO-CNCs were covalently attached to the glucose oxidase using the carbodiimide coupling approach to achieve stable enzyme immobilization, as shown in Fig. 13(a). Operational stability, repeatability, sensitivity, and selectivity were tested for sensors. The sensors were put to work by monitoring the amount of glucose in a fibroblast cell culture's supernatant. The sensors are 5.7 0.3 μA cm^{-2} mM^{-1} sensitive with a linear range of 0.1–2 mM (R^2 = 0.999). The detection limit is 0.004 mM, while the quantification limit is 0.015 mM. The sensor has a shelf life of one month while retaining strong selectivity and 92.3% of the original response time after 30 sequential measurements in a 1 mM standardized glucose solution. Therefore, this paper shows the practical use of the CNCs-based sensor by tracking the glucose utilization of a fibroblast cell culture over several days.

In order to function as dermal and oral glucose biosensors, Tracey *et al.*[233] produced biosensors for potential *in vivo* or dermal application using sulfated and non-sulfated cellulose nanocrystal/magnetite thin films. When glucose is present, the peroxidase-like activity of the biodegradable (N-CNCs)–Fe_3O_4 and (S-CNCs)–Fe_3O_4 hybrid systems is shown by an almost immediate color shift. Both kinds of biosensors are capable of detecting levels of glucose as low as 5 mM, which is the concentration of glucose found in biological fluids; however, (S-CNCs)–Fe_3O_4 is 1.5–2 times more sensitive than (N-CNCs)–Fe_3O_4. Hybrid catalytic efficiency is more evident under acidic conditions and at room temperature. Therefore, the hybrids may measure glucose levels using perspiration and saliva, two non-blood body fluids with relatively low glucose levels and a tendency to be mild to moderately acidic.

4.5.3. CNCs-based enzyme sensors. In many applications, notably in the biomedical industry, the capacity of a biosensor to identify enzymes in trace amounts is essential. Since enzyme quantities change with pathological circumstances, enzymes may be utilized as disease markers.[245] The most popular techniques for detecting enzymes rely on the reducing sugars that are created during enzymatic hydrolysis. On the foundation of this idea, Guyomard-Lack *et al.*[237] created CNCs-based multilayered xyloglucan (XG) films to measure cellulase activity. The films were made layer by layer by either dip coating or spin coating. The original color of the film would depend on its initial thickness. However, the thickness decreases when XG is broken down by cellulase and causes a color shift that can be seen with the naked eye. It offers visual enzyme detection and uses careful thickness and architectural control to measure the

Open Access Article. Published on 08 Febwaliyo 2024. Downloaded on 12/09/2024 22:53:41.
This article is licensed under a Creative Commons Attribution-NonCommercial 3.0 Unported Licence.

enzyme concentration quantitatively. The concentration of CNCs may be changed to achieve this.

Elevated human neutrophil elastase (HNE), a damaging protease, has been suggested as a biomarker for persistent wounds. To reduce HNE levels, a variety of wound treatment techniques have been created. In treating chronic wounds, the biological identification of HNE as a marker or an *in situ* colorimetric additive to chronic wound dressings has potential benefits. Edward and his colleagues[235] described employing peptide-conjugated cotton CNCs as a colorimetric method for detecting HNE. *n*-Succinyl–alanine–alanine–valine–*para*-nitroanilide (Suc–Ala–Ala–Val–pNA), an HNE tripeptide substrate, was covalently linked to glycine esterified CNCs for this purpose and its colorimetric HNE sensor activity was compared with a corresponding tetrapeptide analogue. When compared to analogues synthesized on paper, visible HNE activity on CCN tripeptide conjugates was substantially greater. *para*-Nitroaniline (pNA) was released by an enzyme from the succinyl–Ala–Ala–Val–pNA glycine–CCN compound, and the chromogen's visible absorption was improved by amplifying the pNA's colorimetric response. The capacity of two color-amplifying dyes that interact with pNA to enhance the visual sensor response to HNE activity was contrasted. With CCN tripeptide conjugates, colorimetric HNE detection was sensitive at previously reported HNE levels in chronic wound fluid (0.05 U mL^{-1} HNE). In order to simulate the filtration of HNE and chromogen (pNA) from a model wound dressing surface before and after sensor reactivity, the HNE sensor and the chromogen amplifying dyes were interfaced with 50 and 10 kD dialysis cellulose membranes (DCM). With the CCN-tripeptide conjugate interfaced at the DCM surface distant and proximal to a dressing surface, the detection sensitivity to HNE activity was evaluated. The 10 kD membrane filtration of pNA and subsequent reaction with amplifying dyes provided the best performance for the HNE sensor interface located close to the dressing surface. The 10 kD cellulose membrane interface did not affect the elastase sensor activity's sensitivity to 0.05 U mL^{-1} HNE. The performance, design, and surface characteristics of nanocellulose for the biosensor technique are examined.

Based on the aforementioned reports, it can be deduced that CNCs are attractive for sensing applications due to their biodegradability, cost-effectiveness, tunable surface hydroxyl groups, and low toxicity. By making minor adjustments to CNCs, one can rectify their deficiencies such as being non-conductive and hydrophilic, thereby enhancing their suitability for biosensing applications. This is an emerging and urgently needed field that requires substantial research attention.

5. Challenges of CNCs-based sensors

The information that has been provided thus far makes it readily apparent that the CNCs-based sensors have a broad range of applicability and can be used in real-time applications. A few roadblocks still need to be cleared before we can proceed. The production of CNCs is a time-consuming operation that must be completed. The procedure is time-consuming and needs to be fine-tuned for each unique type of biomass and supply. The quantification and characterization of surface modifications of CNCs, which mostly rely on elemental analysis, are the issues that pose the greatest amount of difficulty. When doing elemental analysis, only the targeted and available hydroxyl groups are taken into account; the bulk modification of NC is disregarded. When we opt for modifying CNCs, the first thing that must be accomplished is a difficult task: dissolving the CNCs in a way that results in controlled substitution. The alteration is then typically accomplished by dispersing the CNCs in various solvents, which results in an uncontrolled degree of substitution. Additionally, the degree of substitution changes from batch to batch.

As a consequence, the behavior of prepared modified CNCs is altered as a consequence of this. Because of their naturally heterogeneous nature, most CNCs-based composite materials cannot effectively function as sensors due to their lack of homogeneity. In addition, the highly hydrophilic nature of NC makes it challenging to implement the material in sensing applications that take place in non-polar media. It is difficult to maintain control over the size of the prepared CNCs when they are being extracted from raw materials such as trash or lignocellulosic matter. This makes it likely that the aspect ratio will be altered. Because the aspect ratio directly influences the properties of CNCs, the qualities of the finished CNCs will inevitably be inconsistent. The fragility of the prepared CNCs is the primary factor that slows down the deployment of this technology in real-time. However, if we are looking at a material that will be used in real-world applications, it should not have a brittle nature.

In order to have a better understanding of surface morphologies, futuristic techniques need to place more of an emphasis on investigating the crystallinity and morphology of the crystalline zone. The extraction operations that lead to the formation of CNCs include the use of acid, which can be reduced to a minimum by employing more environmentally friendly technologies. In spite of the fact that non-conductive CNCs have been investigated for their sensing applications in electroconductive and resistive sensors, CNCs are still subject to discrimination due to their lack of conductivity. As a result, composite materials and conducting polymers might be investigated further in combination with CNCs for the purpose of developing superior sensing applications. As the science of nanotechnology develops, new types of nano-composites that are based on CNCs are coming into existence. When it comes to managing the shape, homogeneity, and density of nanocellulose in sensing platforms, however, there are a lot of obstacles to overcome. Considering these issues, there is a substantial amount of opportunity for development in working on these gaps to get the most beneficial results feasible from CNCs-based sensors.

6. Conclusions and future aspects

To sum up, it is apparent that CNCs possess the capacity to be reconfigured into an extensive array of sensors that are able to

© 2024 The Author(s). Published by the Royal Society of Chemistry

Open Access Article. Published on 08 Febwaliyo 2024. Downloaded on 12/09/2024 22:53:41.
This article is licensed under a Creative Commons Attribution-NonCommercial 3.0 Unported Licence.

detect a variety of environmental analytes. Bioanalytes such as enzymes, proteins, glucose, compounds, gas/humidity, and ions are included among these analytes. CNCs, along with a variety of other materials, find applications in the fabrication of wearable electronic skin sensors that monitor pressure and temperature, among others. Unexplored is a multitude of combinations and facets pertaining to biosensing applications utilizing CNCs nanocomposites. This review article has presented a comprehensive examination of the functionalization of CNCs through the use of materials, including their application as support matrices or as input-responsive sensor components. CNCs' adaptability and versatility enable the fabrication of novel materials with potential applications in sensing technology. The investigation of efficient sensor materials is conducted by utilizing CNCs-based hybrid platforms to examine a range of production alternatives. The potential exists for CNCs platforms to serve as substitutes for numerous biosensors that are presently dependent on plastic or glass platforms. As a result, owing to their biodegradability, CNCs are gaining popularity as an alternative to plastic platforms in optoelectronics. In addition to electrodes, these platforms comprise additional electrochemical devices. In lieu of plastic, CNCs offer a more advantageous substitute for the construction of wearable sensors.

The utilisation of plastic substrates in ubiquitous electrochemical sensors presents two significant obstacles: perspiration-induced interference and the possibility of allergic reactions. It is essential to observe that wearable sensors that simulate CNCs-based sensors in real-world scenarios are not yet commercially available. Hence, by capitalizing on the functionalization potential of CNCs and their nanometric dimensions, it is possible to fabricate ubiquitous sensor-critical batteries and high-performance green supercapacitors. Furthermore, we have emphasized the noteworthy advancements that have been achieved at the laboratory level with respect to the techniques employed for preparation and extraction. Additionally, it is critical that research into the economical production of CNCs on an industrial scale be prioritized in the near future. Similarly, in order to meet the substantial need for sustainable development, it is critical to give precedence to synthetic and fabrication processes that are environmentally friendly and sustainable in nature.

Conflicts of interest

There are no conflicts to declare.

Acknowledgements

The author, Shiva Singh, would like to thank his PhD supervisors, Prof. Pradip K. Maji and Prof. Kaushik Ghosh, who helped him during his study at the Department of Polymer and Process Engineering, Indian Institute of Technology (IIT), Roorkee. The author would also like to thank his colleagues and friends who contributed to his study. Finally, the authors Shiva Singh and Shakshi Bhardwaj gratefully acknowledge the Prime Minister Research Fellowship Program with contingency, Government of India for financial support.

References

1 A. Uniyal, G. Srivastava, A. Pal, S. Taya and A. Muduli, *Plasmonics*, 2023, **18**, 735–750.
2 N. Aslam, H. Zhou, E. K. Urbach, M. J. Turner, R. L. Walsworth, M. D. Lukin and H. Park, *Nat. Rev. Phys.*, 2023, **5**, 157–169.
3 Y. S. Rim, S. H. Bae, H. Chen, N. De Marco and Y. Yang, *Adv. Mater.*, 2016, **28**, 4415–4440.
4 K. Chen, W. Gao, S. Emaminejad, D. Kiriya, H. Ota, H. Y. Y. Nyein, K. Takei and A. Javey, *Adv. Mater.*, 2016, **28**, 4397–4414.
5 Y. Cheng, R. Wang, J. Sun and L. Gao, *Adv. Mater.*, 2015, **27**, 7365–7371.
6 S. Takamatsu, T. Lonjaret, E. Ismailova, A. Masuda, T. Itoh and G. G. Malliaras, *Adv. Mater.*, 2016, **28**, 4485–4488.
7 C. Verma, M. Chhajed, S. Singh, M. Sathwane and P. K. Maji, *Colloids Surf., A*, 2022, **655**, 130206.
8 C. Verma, M. Chhajed, S. Singh and P. K. Maji, *ACS Appl. Polym. Mater.*, 2022, **4**, 4047–4068.
9 G. Dandegaonkar, A. Ahmed, L. Sun, B. Adak and S. Mukhopadhyay, *Mater. Adv.*, 2022, **3**, 3766–3783.
10 T. Xu, Q. Song, K. Liu, H. Liu, J. Pan, W. Liu, L. Dai, M. Zhang, Y. Wang, C. Si, H. Du and K. Zhang, *Nano-Micro Lett.*, 2023, **15**, 1–14.
11 R. Xiong, C. Lu, W. Zhang, Z. Zhou and X. Zhang, *Carbohydr. Polym.*, 2013, **95**, 214–219.
12 K. Oksman, A. P. Mathew, D. Bondeson and I. Kvien, *Compos. Sci. Technol.*, 2006, **66**, 2776–2784.
13 W. H. Danial, Z. Abdul Majid, M. N. Mohd Muhid, S. Triwahyono, M. B. Bakar and Z. Ramli, *Carbohydr. Polym.*, 2015, **118**, 165–169.
14 R. M. A. Domingues, M. E. Gomes and R. L. Reis, *Biomacromolecules*, 2014, **15**, 2327–2346.
15 S. Bhardwaj, S. Singh, P. Gupta, N. Choudhary and P. K. Maji, *Int. J. Green Energy*, 2023, DOI: **10.1080/15435075.2023.2253873**.
16 L. Van Hai, H. N. Son and Y. B. Seo, *Cellulose*, 2015, **22**, 1789–1798.
17 L. Van Hai and Y. B. Seo, *Nord. Pulp Pap. Res. J.*, 2017, **32**, 170–178.
18 B. Sun, M. Zhang, Q. Hou, R. Liu, T. Wu and C. Si, *Cellulose*, 2016, **23**, 439–450.
19 K. K. Sadasivuni, A. Kafy, L. Zhai, H. U. Ko, S. Mun and J. Kim, *Small*, 2015, **11**, 994–1002.
20 V. Favier, H. Chanzy and J. Y. Cavaillé, *Macromolecules*, 1995, **28**, 6365–6367.
21 Z. Hosseinidoust, M. N. Alam, G. Sim, N. Tufenkji and T. G. M. Van De Ven, *Nanoscale*, 2015, **7**, 16647–16657.
22 P. Sarrazin, D. Chaussy, O. Stephan, L. Vurth and D. Beneventi, *Colloids Surf., A*, 2009, **349**, 83–89.

Open Access Article. Published on 08 Febwaliyo 2024. Downloaded on 12/09/2024 22:53:41.
This article is licensed under a Creative Commons Attribution-NonCommercial 3.0 Unported Licence.

23 M. J. Bonné, K. J. Edler, J. G. Buchanan, D. Wolverson, E. Psillakis, M. Helton, W. Thielemans and F. Marken, *J. Phys. Chem. C*, 2008, **112**, 2660–2666.
24 S. Wang, J. Sun, Y. Jia, L. Yang, N. Wang, Y. Xianyu, W. Chen, X. Li, R. Cha and X. Jiang, *Biomacromolecules*, 2016, **17**, 2472–2478.
25 S. Singh, S. Bhardwaj, C. Verma, M. Chhajed, K. Balayan, K. Ghosh and P. K. Maji, *J. Mol. Liq.*, 2022, **366**, DOI: 10.1016/j.molliq.2022.120326.
26 J. E. Sanders, L. Wang, G. Brinkley and D. J. Gardner, *Cellulose*, 2023, **30**, 6303–6315.
27 H. Wu, X. Liu, X. Hua and J. Zhang, *Ind. Crops Prod.*, 2023, **202**, 117008.
28 Y. F. Yan, X. B. Liang, Y. L. Feng, L. F. Shi, R. P. Chen, J. Z. Guo and Y. Guan, *Carbohydr. Polym.*, 2023, **320**, 121251.
29 V. C. Agbakoba, P. Hlangothi, J. Andrew and M. J. John, *Nanoscale Adv.*, 2023, **5**, 4447–4463.
30 H. Kwak, H. Kim, S. A. Park, M. Lee, M. Jang, S. B. Park, S. Y. Hwang, H. J. Kim, H. Jeon, J. M. Koo, J. Park and D. X. Oh, *Adv. Sci.*, 2023, **10**, 2205554.
31 N. A. Zabidi, N. N. Zainal, I. S. M. A. Tawakkal, M. S. Mohd Basri, S. H. Ariffin and M. N. Naim, *Int. J. Biol. Macromol.*, 2023, **251**, 126212.
32 X. Zhang, J. Zhou, W. Huang, C. Wu and J. Nan, *Cellulose*, 2023, **30**, 1517–1532.
33 C. E. Boott, L. Shi, Z. Li, W. Y. Hamad and M. J. MacLachlan, *Liq. Cryst.*, 2023, **50**, 1143–1150.
34 X. Fan, L. Zhang, F. Dong, H. Liu and X. Xu, *Carbohydr. Polym.*, 2023, **308**, 120654.
35 T. Dolui, T. S. Natarajan, S. Aiswarya, J. Chanda, P. Ghosh, R. Mukhopadhyay, S. Wießner, G. Heinrich, A. Das and S. S. Banerjee, *Adv. Eng. Mater.*, 2023, **25**, 2300584.
36 S. Singh, G. L. Dhakar, B. P. Kapgate, P. K. Maji, C. Verma, M. Chhajed, K. Rajkumar and C. Das, *Polym. Adv. Technol.*, 2020, **31**, 3059–3069.
37 M. Guo, R. Xiao, N. Prempeh, D. Liu, J. Fu, Y. Cai, A. Oumaima, T. Iimaa and U. Surenjav, *Ind. Crops Prod.*, 2023, **192**, 116007.
38 F. Pena-Pereira, I. Lavilla, I. de la Calle, V. Romero and C. Bendicho, *Anal. Bioanal. Chem.*, 2023, **415**, 4039–4060.
39 J. Chen, Z. Ling, X. Wang, X. Ping, Y. Xie, H. Ma, J. Guo and Q. Yong, *Chem. Eng. J.*, 2023, **466**, 143148.
40 M. Lin, V. S. Raghuwanshi, C. Browne, G. P. Simon and G. Garnier, *J. Colloid Interface Sci.*, 2023, **629**, 694–704.
41 H. Cho, G. Lee, V. V. Tsukruk and S. Kim, *Cellulose*, 2023, **30**, 6435–6456.
42 C. Zheng, K. Lu, Y. Lu, S. Zhu, Y. Yue, X. Xu, C. Mei, H. Xiao, Q. Wu and J. Han, *Carbohydr. Polym.*, 2020, **250**, 116905.
43 J. Xing, P. Tao, Z. Wu, C. Xing, X. Liao and S. Nie, *Carbohydr. Polym.*, 2019, **207**, 447–459.
44 S. Zhu, H. Sun, Y. Lu, S. Wang, Y. Yue, X. Xu, C. Mei, H. Xiao, Q. Fu and J. Han, *ACS Appl. Mater. Interfaces*, 2021, **13**, 59142–59153.
45 D. Hu, K. H. Lin, Y. Xu, M. Kajiyama, M. A. Neves, K. Ogawa and T. Enomae, *Cellulose*, 2021, **28**, 9705–9724.
46 S. Mukherjee, H. Ramireddy, A. Baidya, A. K. Amala, C. Sudhakar, B. Mondal, L. Philip and T. Pradeep, *ACS Sustain. Chem. Eng.*, 2020, **8**, 139–147.
47 C. Zheng, Y. Yue, L. Gan, X. Xu, C. Mei and J. Han, *Nanomaterials*, 2019, **9**, 937.
48 A. Subhedar, S. Bhadauria, S. Ahankari and H. Kargarzadeh, *Int. J. Biol. Macromol.*, 2021, **166**, 587–600.
49 S. Kumar, M. R. Ngasainao, D. Sharma, M. Sengar, A. P. S. Gahlot, S. Shukla and P. Kumari, *Carbohydr. Polym.*, 2022, **298**, 120052.
50 M. N. F. Norrrahim, N. A. Mohd Kasim, V. F. Knight, F. A. Ujang, N. Janudin, M. A. I. Abdul Razak, N. A. A. Shah, S. A. M. Noor, S. H. Jamal, K. K. Ong and W. M. Z. Wan Yunus, *Mater. Adv.*, 2021, **2**, 1485–1506.
51 F. Ji, Z. Sun, T. Hang, J. Zheng, X. Li, G. Duan, C. Zhang and Y. Chen, *Compos. Commun.*, 2022, **35**, 101351.
52 P. Lv, X. Lu, L. Wang and W. Feng, *Adv. Funct. Mater.*, 2021, **31**, 2104991.
53 L. Dai, Y. Wang, X. Zou, Z. Chen, H. Liu and Y. Ni, *Small*, 2020, **16**, 1906567.
54 V. Gupta, D. Ramakanth, C. Verma, P. K. Maji and K. K. Gaikwad, *Biomass Convers. Biorefinery*, 2021, **1**, 1–12.
55 D. Ramakanth, S. Singh, P. K. Maji, Y. S. Lee and K. K. Gaikwad, *Environ. Chem. Lett.*, 2021, **19**, 3597–3608.
56 P. P. Sharma, S. Bhardwaj, A. Sethi, V. K. Goel, M. Grishina, Poonam and B. Rathi, *Carbohydr. Res.*, 2022, **522**, 108703.
57 A. Kafy, K. K. Sadasivuni, H. C. Kim, A. Akther and J. Kim, *Phys. Chem. Chem. Phys.*, 2015, **17**, 5923–5931.
58 Suhas, V. K. Gupta, P. J. M. Carrott, R. Singh, M. Chaudhary and S. Kushwaha, *Bioresour. Technol.*, 2016, **216**, 1066–1076.
59 J. George and S. N. Sabapathi, *Nanotechnol., Sci. Appl.*, 2015, **8**, 45–54.
60 P. Tingaut, T. Zimmermann and G. Sèbe, *J. Mater. Chem.*, 2012, **22**, 20105–20111.
61 T. Huber, S. Pang and M. P. Staiger, *Composites, Part A*, 2012, **43**, 1738–1745.
62 J. Kim, S. Yun and Z. Ounaies, *Macromolecules*, 2006, **39**, 4202–4206.
63 J. H. Kim, S. Mun, H. U. Ko, G. Y. Yun and J. Kim, *Nanotechnology*, 2014, **25**, 092001.
64 M. A. S. Azizi Samir, F. Alloin and A. Dufresne, *Biomacromolecules*, 2005, **6**, 612–626.
65 F. Li, E. Mascheroni and L. Piergiovanni, *Packag. Technol. Sci.*, 2015, **28**, 475–508.
66 P. Gupta, C. Verma and P. K. Maji, *J. Supercrit. Fluids*, 2019, **152**, 104537.
67 M. Chhajed, C. Verma, M. Sathawane, S. Singh and P. K. Maji, *Mar. Pollut. Bull.*, 2022, **180**, 113790.
68 M. Sathwane, M. Chhajed, C. Verma, K. K. Gaikwad and P. K. Maji, *Polym. Compos.*, 2023, **44**, 492–504.
69 L. H. Nguyen, S. Naficy, R. Chandrawati and F. Dehghani, *Adv. Mater. Interfaces*, 2019, **6**, 1900424.
70 R. J. Moon, A. Martini, J. Nairn, J. Simonsen and J. Youngblood, *Chem. Soc. Rev.*, 2011, **40**, 3941–3994.

© 2024 The Author(s). Published by the Royal Society of Chemistry

Open Access Article. Published on 08 Febwaliyo 2024. Downloaded on 12/09/2024 22:53:41.
This article is licensed under a Creative Commons Attribution-NonCommercial 3.0 Unported Licence.

71 A. D. French, N. R. Bertoniere, O. A. Battista, J. A. Cuculo and D. G. Gray, *Kirk-Othmer Encycl. Chem. Technol.*, 2000, DOI: 10.1002/0471238961.0305121206180514.A01.
72 K. H. Gardner and J. Blackwell, *Biopolymers*, 1974, **13**, 1975–2001.
73 P. Liu, B. Pang, S. Dechert, X. C. Zhang, L. B. Andreas, S. Fischer, F. Meyer and K. Zhang, *Angew. Chem., Int. Ed.*, 2020, **59**, 3218–3225.
74 S. Bhardwaj, S. Singh, R. S. Meda, S. Jain and P. K. Maji, *Biomass Convers. Biorefinery*, 2023, **1**, 1–14.
75 D. Klemm, F. Kramer, S. Moritz, T. Lindström, M. Ankerfors, D. Gray and A. Dorris, *Angew. Chem., Int. Ed.*, 2011, **50**, 5438–5466.
76 R. S. Meda, S. Jain, S. Singh, C. Verma, U. Nandi and P. K. Maji, *Ind. Crops Prod.*, 2022, **186**, 115197.
77 M. Chhajed, C. Yadav, A. K. Agrawal and P. K. Maji, *Carbohydr. Polym.*, 2019, **226**, 115286.
78 C. Verma, M. Chhajed, P. Gupta, S. Roy and P. K. Maji, *Int. J. Biol. Macromol.*, 2021, **175**, 242–253.
79 X. Xu, F. Liu, L. Jiang, J. Y. Zhu, D. Haagenson and D. P. Wiesenborn, *ACS Appl. Mater. Interfaces*, 2013, **5**, 2999–3009.
80 P. Gupta, A. Pandey, K. K. Gaikwad, S. Roy and P. K. Maji, *Polym. Eng. Sci.*, 2021, **61**, 1220–1231.
81 L. G. Greca, J. Lehtonen, B. L. Tardy, J. Guo and O. J. Rojas, *Mater. Horiz.*, 2018, **5**, 408–415.
82 H. P. S. Abdul Khalil, Y. Davoudpour, M. N. Islam, A. Mustapha, K. Sudesh, R. Dungani and M. Jawaid, *Carbohydr. Polym.*, 2014, **99**, 649–665.
83 D. Klemm, D. Schumann, F. Kramer, N. Hebler, D. Koth and B. Sultanova, *Macromol. Symp.*, 2009, **280**, 60–71.
84 D. Klemm, K. Petzold-Welcke, F. Kramer, T. Richter, V. Raddatz, W. Fried, S. Nietzsche, T. Bellmann and D. Fischer, *Carbohydr. Polym.*, 2021, **254**, 117313.
85 C. Miao, L. Reid and W. Y. Hamad, *Appl. Mater. Today*, 2021, **24**, 101082.
86 J. Fan, M. Xu, Y. T. Xu, W. Y. Hamad, Z. Meng and M. J. MacLachlan, *Chem. Eng. J.*, 2023, **457**, 141175.
87 J. Peng, H. Zhang, Q. Zheng, C. M. Clemons, R. C. Sabo, S. Gong, Z. Ma and L. S. Turng, *Nanoscale*, 2017, **9**, 1428–1433.
88 S. Roy, H. U. Ko, P. K. Maji, L. Van Hai and J. Kim, *Chem. Eng. J.*, 2020, **385**, 123723.
89 S. P. Bangar, M. M. Harussani, R. A. Ilyas, A. O. Ashogbon, A. Singh, M. Trif and S. M. Jafari, *Food Hydrocoll.*, 2022, **130**, 107689.
90 C. Nitesh, S. Singh, S. Bhardwaj, S. Gupta, U. Nandi, R. Chandra and P. K. Maji, *Carbohydr. Polym. Technol. Appl.*, 2024, **7**, DOI: 10.1016/j.carpta.2023.100416.
91 B. K. Mahur, A. Ahuja, S. Singh, P. K. Maji and V. K. Rastogi, *Int. J. Biol. Macromol.*, 2023, **253**, 126657.
92 S. Singh, S. Bhardwaj, R. S. Meda, C. Verma, M. Chhajed, K. Ghosh and P. K. Maji, *Int. J. Biol. Macromol.*, 2023, **242**, 124507.
93 I. K. R. Dias, B. K. Lacerda and V. Arantes, *Int. J. Biol. Macromol.*, 2023, **242**, 125053.
94 G. Abdalla Suliman Haron, H. Mahmood, M. Hilmi Bin Noh and M. Moniruzzaman, *J. Mol. Liq.*, 2022, **368**, 120591.
95 L. P. Novo, J. Bras, A. García, N. Belgacem and A. A. S. Curvelo, *ACS Sustainable Chem. Eng.*, 2015, **3**, 2839–2846.
96 D. Trache, M. H. Hussin, M. K. M. Haafiz and V. K. Thakur, *Nanoscale*, 2017, **9**, 1763–1786.
97 R. Requena, A. Jiménez-Quero, M. Vargas, R. Moriana, A. Chiralt and F. Vilaplana, *ACS Sustainable Chem. Eng.*, 2019, **7**, 6275–6286.
98 H. Abushammala, I. Krossing and M. P. Laborie, *Carbohydr. Polym.*, 2015, **134**, 609–616.
99 K. Zhang, P. Sun, H. Liu, S. Shang, J. Song and D. Wang, *Carbohydr. Polym.*, 2016, **138**, 237–243.
100 J. Lamaming, R. Hashim, O. Sulaiman, C. P. Leh, T. Sugimoto and N. A. Nordin, *Carbohydr. Polym.*, 2015, **127**, 202–208.
101 Y. Tang, X. Shen, J. Zhang, D. Guo, F. Kong and N. Zhang, *Carbohydr. Polym.*, 2015, **125**, 360–366.
102 V. K. Thakur, *Nanocellul. Polym. Nanocompos.*, 2014, **9781118871**, 1–513.
103 N. F. Vasconcelos, J. P. A. Feitosa, F. M. P. da Gama, J. P. S. Morais, F. K. Andrade, M. de S. M. de Souza Filho and M. de F. Rosa, *Carbohydr. Polym.*, 2017, **155**, 425–431.
104 M. Jonoobi, R. Oladi, Y. Davoudpour, K. Oksman, A. Dufresne, Y. Hamzeh and R. Davoodi, *Cellulose*, 2015, **22**, 935–969.
105 F. Bettaieb, R. Khiari, A. Dufresne, M. F. Mhenni and M. N. Belgacem, *Carbohydr. Polym.*, 2015, **123**, 99–104.
106 V. Baheti and J. Militky, *Fibers Polym.*, 2013, **14**, 133–137.
107 Y. Yu and H. Wu, *AIChE J.*, 2011, **57**, 793–800.
108 M. Pääkko, M. Ankerfors, H. Kosonen, A. Nykänen, S. Ahola, M. Österberg, J. Ruokolainen, J. Laine, P. T. Larsson, O. Ikkala and T. Lindström, *Biomacromolecules*, 2007, **8**, 1934–1941.
109 T. Zimmermann, N. Bordeanu and E. Strub, *Carbohydr. Polym.*, 2010, **79**, 1086–1093.
110 Q. Cheng, S. Wang and T. G. Rials, *Composites., Part A*, 2009, **40**, 218–224.
111 C. C. Kwan, M. Ghadiri, D. G. Papadopoulos and A. C. Bentham, *Chem. Eng. Technol.*, 2003, **26**, 185–190.
112 D. Yang, X. W. Peng, L. X. Zhong, X. F. Cao, W. Chen and R. C. Sun, *Cellulose*, 2013, **20**, 2427–2437.
113 W. Li, J. Yue and S. Liu, *Ultrason. Sonochem.*, 2012, **19**, 479–485.
114 K. N. Mohd Amin, P. K. Annamalai, I. C. Morrow and D. Martin, *RSC Adv.*, 2015, **5**, 57133–57140.
115 X. Cao, B. Ding, J. Yu and S. S. Al-Deyab, *Carbohydr. Polym.*, 2012, **90**, 1075–1080.
116 Y. Okita, T. Saito and A. Isogai, *Biomacromolecules*, 2010, **11**, 1696–1700.
117 S. R. Anderson, D. Esposito, W. Gillette, J. Y. Zhu, U. Baxa and S. E. McNeil, *Tappi J.*, 2014, **13**, 35–42.
118 A. Dufresne, *Nanocellulose: From nature to high performance tailored materials*, De Gruyter Mouton, 2012, vol. 67.
119 X. Chen, X. Deng, W. Shen and L. Jiang, *BioResources*, 2012, **7**, 4237–4248.

Open Access Article. Published on 08 Febwaliyo 2024. Downloaded on 12/09/2024 22:53:41.
This article is licensed under a Creative Commons Attribution-NonCommercial 3.0 Unported Licence.

120 X. Y. Tan, S. B. Abd Hamid and C. W. Lai, *Biomass Bioenergy*, 2015, **81**, 584–591.
121 Q. Zhang, K. De Oliveira Vigier, S. Royer and F. Jérôme, *Chem. Soc. Rev.*, 2012, **41**, 7108–7146.
122 H. Wang, J. Li, X. Zeng, X. Tang, Y. Sun, T. Lei and L. Lin, *Cellulose*, 2020, **27**, 1301–1314.
123 M. Lee, M. H. Heo, H. Lee, H. H. Lee, H. Jeong, Y. W. Kim and J. Shin, *Green Chem.*, 2018, **20**, 2596–2610.
124 L. P. Novo, J. Bras, A. García, N. Belgacem and A. A. da S. Curvelo, *Ind. Crops Prod.*, 2016, **93**, 88–95.
125 J. F. Revol, H. Bradford, J. Giasson, R. H. Marchessault and D. G. Gray, *Int. J. Biol. Macromol.*, 1992, **14**, 170–172.
126 L. Onsager, *Ann. N. Y. Acad. Sci.*, 1949, **51**, 627–659.
127 M. Mitov, *Adv. Mater.*, 2012, **24**, 6260–6276.
128 H. de Vries, *Acta Crystallogr.*, 1951, **4**, 219–226.
129 M. D. Xue, T. Kimura, J. F. Revol and D. G. Gray, *Langmuir*, 1996, **12**, 2076–2082.
130 J. F. Revol, L. Godbout, X. M. Dong, D. G. Gray, H. Chanzy and G. Maret, *Liq. Cryst.*, 1994, **16**, 127–134.
131 S. Beck-Candanedo, M. Roman and D. G. Gray, *Biomacromolecules*, 2005, **6**, 1048–1054.
132 A. G. Dumanli, H. M. Van Der Kooij, G. Kamita, E. Reisner, J. J. Baumberg, U. Steiner and S. Vignolini, *ACS Appl. Mater. Interfaces*, 2014, **6**, 12302–12306.
133 Q. Chen, P. Liu, F. Nan, L. Zhou and J. Zhang, *Biomacromolecules*, 2014, **15**, 4343–4350.
134 M. K. Khan, M. Giese, M. Yu, J. A. Kelly, W. Y. Hamad and M. J. Maclachlan, *Angew. Chem., Int. Ed.*, 2013, **52**, 8921–8924.
135 A. V. Samrot, K. T. Ngaakudzwe, D. Rajalakshmi, P. Prakash, S. Suresh Kumar, M. Chandramohan, D. Alex Anand, J. Lilly Mercy, Y. Simon and S. Saigeetha, *Adv. Mater. Sci. Eng.*, 2022, DOI: **10.1155/2022/7314694**.
136 D. Ramakanth, S. Singh, S. Bhardwaj, R. S. Meda, K. K. Gaikwad and P. K. Maji, *ACS Appl. Polym. Mater.*, 2023, **5**, 9888–9897.
137 T. S. George, S. A. Muhammadaly, B. Parambath Kanoth, T. Joseph, M. D. Chemmarickal Dominic, N. George, V. Balachandrakurupp and H. John, *Packag. Technol. Sci.*, 2022, **35**, 163–174.
138 M. L. Hassan, Bagasse and rice straw nanocellulosic materials and their applications, *Handbook of Polymer Nanocomposites*, *Processing, Performance and Application*, 2015, vol. C.
139 L. Cao, J. Huang and Y. Chen, *ACS Sustainable Chem. Eng.*, 2018, **6**, 14802–14811.
140 O. Somseemee, P. Saeoui, F. T. Schevenels and C. Siriwong, *Sci. Rep.*, 2022, **12**, 1–13.
141 J. M. Jardin, Z. Zhang, G. Hu, K. C. Tam and T. H. Mekonnen, *Int. J. Biol. Macromol.*, 2020, **152**, 428–436.
142 G. Siqueira, H. Abdillahi, J. Bras and A. Dufresne, *Cellulose*, 2010, **17**, 289–298.
143 M. Pirzada and Z. Altintas, *Fundam. Sens. Technol. Princ. Nov. Des.*, 2023, 3–16.
144 E. M. Southern, *J. Mol. Biol.*, 1975, **98**, 503–517.
145 B. Schyrr, S. Pasche, G. Voirin, C. Weder, Y. C. Simon and E. J. Foster, *ACS Appl. Mater. Interfaces*, 2014, **6**, 12674–12683.
146 L. Chen, W. Cao, N. Grishkewich, R. M. Berry and K. C. Tam, *J. Colloid Interface Sci.*, 2015, **450**, 101–108.
147 T. Wu, J. Li, J. Li, S. Ye, J. Wei and J. Guo, *J. Mater. Chem. C*, 2016, **4**, 9687–9696.
148 J. Cao, X. Zhang, X. Wu, S. Wang and C. Lu, *Carbohydr. Polym.*, 2016, **140**, 88–95.
149 S. Dai, N. Prempeh, D. Liu, Y. Fan, M. Gu and Y. Chang, *Carbohydr. Polym.*, 2017, **174**, 531–539.
150 W. Wu, R. Song, Z. Xu, Y. Jing, H. Dai and G. Fang, *Sens. Actuators, B*, 2018, **275**, 490–498.
151 L. Han, S. Cui, H. Y. Yu, M. Song, H. Zhang, N. Grishkewich, C. Huang, D. Kim and K. M. C. Tam, *ACS Appl. Mater. Interfaces*, 2019, **11**, 44642–44651.
152 A. Ivanova, B. Frka-Petesic, A. Paul, T. Wagner, A. N. Jumabekov, Y. Vilk, J. Weber, J. Schmedt Auf Der Günne, S. Vignolini, M. Tiemann, D. Fattakhova-Rohlfing and T. Bein, *ACS Appl. Mater. Interfaces*, 2020, **12**, 12639–12647.
153 X. Ye, Y. Kang and J. Zhou, *Cellulose*, 2020, **27**, 5197–5210.
154 P. C. Lai and S. S. Yu, *Polymers*, 2021, **13**, 1–17.
155 X. Sun, J. Li, Q. He, Y. Xue, Y. Bai, Y. Yang, X. Wang, S. Wang and R. Li, *RSC Adv.*, 2022, **12**, 16798–16804.
156 J. Huang, Z. Li, T. Kang, W. Wei, F. Liu, X. Xu and Z. Liu, *Compos. Struct.*, 2023, **320**, 117231.
157 Q. Li, C. He, C. Wang, Y. Huang, J. Yu, C. Wang, W. Li, X. Zhang, F. Zhang and G. Qing, *Small*, 2023, **19**, 2207932.
158 B. Li, Y. Chen, W. Wu, X. Cao and Z. Luo, *Carbohydr. Polym.*, 2023, **317**, 121092.
159 X. Wei, T. Lin, L. Wang, J. Lin and X. Yin, *Int. J. Biol. Macromol.*, 2023, **235**, 123805.
160 J. T. Orasugh, V. Saasa, S. S. Ray and B. Mwakikunga, *Int. J. Biol. Macromol.*, 2023, **241**, 124514.
161 Z. Hanif, Z. A. Khan, M. Z. Tariq, D. Choi and S. J. Park, *Dyes Pigm.*, 2021, **196**, 109732.
162 N. Mohammed, A. Baidya, V. Murugesan, A. A. Kumar, M. A. Ganayee, J. S. Mohanty, K. C. Tam and T. Pradeep, *ACS Sustainable Chem. Eng.*, 2016, **4**, 6167–6176.
163 R. Song, Q. Zhang, Y. Chu, L. Zhang, H. Dai and W. Wu, *Cellulose*, 2019, **26**, 9553–9565.
164 Y. J. Zhang, X. Z. Ma, L. Gan, T. Xia, J. Shen and J. Huang, *Cellulose*, 2018, **25**, 5831–5842.
165 L. L. Zhang, Q. Li, J. Zhou and L. L. Zhang, *Macromol. Chem. Phys.*, 2012, **213**, 1612–1617.
166 Y. Han, X. Wu, X. Zhang, Z. Zhou and C. Lu, *ACS Sustainable Chem. Eng.*, 2016, **4**, 5667–5673.
167 H. Chen, J. Huang, B. Hao, B. Yang, S. Chen, G. Yang and J. Xu, *Carbohydr. Polym.*, 2019, **224**, 115198.
168 J. Chen, Z. Zhou, Z. Chen, W. Yuan and M. Li, *New J. Chem.*, 2017, **41**, 10272–10280.
169 Z. Karim, A. P. Mathew, V. Kokol, J. Wei and M. Grahn, *RSC Adv.*, 2016, **6**, 20644–20653.
170 C. Peng, T. Long, X. Huang, M. Ouyang, H. Luo, W. Xu, D. Xu and Q. Lin, *Ind. Crops Prod.*, 2022, **189**, 115743.
171 D. P. Dubal, N. R. Chodankar, D. H. Kim and P. Gomez-Romero, *Chem. Soc. Rev.*, 2018, **47**, 2065–2129.

© 2024 The Author(s). Published by the Royal Society of Chemistry

Open Access Article. Published on 08 Febwaliyo 2024. Downloaded on 12/09/2024 22:53:41.
This article is licensed under a Creative Commons Attribution-NonCommercial 3.0 Unported Licence.

172 R. Thangarasu, E. Thangavel, J. Chandrasekaran and O. N. Balasundaram, *J. Mater. Sci.: Mater. Electron.*, 2019, **30**, 4238–4249.
173 X. Tong, X. Zhang, J. Li and H. Wang, *J. Mater. Sci.: Mater. Electron.*, 2021, **32**, 23566–23577.
174 G. Zhao, Y. Zhang, S. Zhai, J. Sugiyama, M. Pan, J. Shi and H. Lu, *ACS Appl. Mater. Interfaces*, 2020, **12**, 17833–17844.
175 W. Song, J. K. Lee, M. S. Gong, K. Heo, W. J. Chung and B. Y. Lee, *ACS Appl. Mater. Interfaces*, 2018, **10**, 10353–10361.
176 P. Sukhavattanakul and H. Manuspiya, *Carbohydr. Polym.*, 2020, **230**, 115566.
177 K. K. Sadasivuni, D. Ponnamma, H. U. Ko, H. C. Kim, L. Zhai and J. Kim, *Sens. Actuators, B*, 2016, **233**, 633–638.
178 Y. Zhao, G. Gao, D. Liu, D. Tian, Y. Zhu and Y. Chang, *Carbohydr. Polym.*, 2017, **174**, 39–47.
179 V. L. Prasanna, H. Mamane, V. K. Vadivel and D. Avisar, *J. Hazard. Mater.*, 2020, **384**, 121396.
180 J. F. Olorunyomi, S. T. Geh, R. A. Caruso and C. M. Doherty, *Mater. Horiz.*, 2021, **8**, 2387–2419.
181 K. Yao, Q. Meng, V. Bulone, Q. Zhou, K. Yao, Q. Meng, V. Bulone and Q. Zhou, *Adv. Mater.*, 2017, **29**, 1701323.
182 L. Bai, Z. L. Wang, Y. D. He, F. Song, X. L. Wang and Y. Z. Wang, *ACS Sustainable Chem. Eng.*, 2020, **8**, 18484–18491.
183 Y. Gao and Z. Jin, *ACS Sustainable Chem. Eng.*, 2018, **6**, 6192–6202.
184 E. Núñez-Carmona, A. Bertuna, M. Abbatangelo, V. Sberveglieri, E. Comini and G. Sberveglieri, *Mater. Lett.*, 2019, **237**, 69–71.
185 Y. Tang, X. Xu, H. Du, H. Zhu, D. Li, D. Ao, Y. Guo, Y. Q. Fu and X. Zu, *Sens. Actuators, A*, 2020, **301**, 111792.
186 C. Y. Hu, L. Bai, F. Song, Y. Z. L. Wang and Y. Z. L. Wang, *Carbohydr. Polym.*, 2022, **296**, 119929.
187 M. Giese, L. K. Blusch, M. K. Khan, W. Y. Hamad and M. J. Maclachlan, *Angew. Chem., Int. Ed.*, 2014, **53**, 8880–8884.
188 Q. Bi, S. Dong, Y. Sun, X. Lu and L. Zhao, *Anal. Biochem.*, 2016, **508**, 50–57.
189 Y. Zheng, L. Zhang and B. Duan, *Carbohydr. Polym.*, 2022, **295**, 119866.
190 S. A. Ogundare and W. E. van Zyl, *Colloids Surf., A*, 2019, **570**, 156–164.
191 T. Hiratani, O. Kose, W. Y. Hamad and M. J. Maclachlan, *Mater. Horiz.*, 2018, **5**, 1076–1081.
192 Y. Wang, L. Zhang, J. Zhou and A. Lu, *ACS Appl. Mater. Interfaces*, 2020, **12**, 7631–7638.
193 J. He, K. Bian, N. Li and G. Piao, *ACS Sustainable Chem. Eng.*, 2019, **7**, 12369–12375.
194 H. Xu, X. Liu, J. Qin, L. Dong, S. Gao, F. Hou, L. Zhong, T. Jiang and N. Lin, *Microchem. J.*, 2021, **168**, 106494.
195 M. A. Khalilzadeh, S. Tajik, H. Beitollahi and R. A. Venditti, *Ind. Eng. Chem. Res.*, 2020, **59**, 4219–4228.
196 A. Kafy, A. Akther, M. I. R. Shishir, H. C. Kim, Y. Yun and J. Kim, *Sens. Actuators, A*, 2016, **247**, 221–226.
197 H. Li, H. Zhu, Z. Quan, Z. Chen, L. Wang and H. He, *Int. J. Biol. Macromol.*, 2023, **224**, 1079–1090.
198 H. Liu, H. Li, S. Xia, S. Yu, Y. Duan, L. Wang, H. Zhu and H. He, *Chem. Eng. J.*, 2023, **454**, 140456.
199 W. E. Faradillawan Khalid, M. Nasir Mat Arip, L. Jasmani and Y. H. Lee, *Sensors*, 2019, **19**, 2726.
200 J. Fan, S. Liang, M. Zhang, G. Xu, J. Fan, S. Liang, M. Zhang and G. Xu, *J. Bioresour. Bioprod.*, 2018, **3**, 30–34.
201 H. Deng, Q. Chen, F. Xie, C. Zhao, J. Pan, Q. Cheng and C. Zhang, *Carbohydr. Polym.*, 2023, **302**, 120313.
202 J. Wang, Q. Cheng, S. Feng, L. Zhang and C. Chang, *J. Mater. Chem. C*, 2021, **9**, 6344–6350.
203 K. Maity, A. Mondal and M. C. Saha, *ACS Appl. Mater. Interfaces*, 2023, **15**, 13956–13970.
204 Y. He, L. Lu, Y. Lin, R. Li, Y. Yuan, X. Lu, Y. Zou, W. Zhou, Z. Wang and J. Li, *Int. J. Biol. Macromol.*, 2022, **218**, 900–908.
205 S. Li, Y. He, X. Ye, X. Fu, Y. Hou, H. Tian, J. Huang and L. Gan, *Carbohydr. Polym.*, 2022, **298**, 120099.
206 C. E. Boott, A. Tran, W. Y. Hamad and M. J. MacLachlan, *Angew. Chem., Int. Ed.*, 2020, **59**, 226–231.
207 S. Chen, Y. Chen, D. Li, Y. Xu and F. Xu, *ACS Appl. Mater. Interfaces*, 2021, **13**, 8754–8763.
208 Y. Cao, L. Lewis, W. Y. Hamad and M. J. MacLachlan, *Adv. Mater.*, 2019, **31**, 1808186.
209 O. Kose, A. Tran, L. Lewis, W. Y. Hamad and M. J. MacLachlan, *Nat. Commun.*, 2019, **10**, 1–7.
210 J. Zheng, Y. Sun, S. Yang, Z. Li, X. Tang, X. Zeng and L. Lin, *New J. Chem.*, 2022, **4**, 20900–20908.
211 O. Kose, C. E. Boott, W. Y. Hamad and M. J. Maclachlan, *Macromolecules*, 2019, **52**, 5317–5324.
212 J. Chen, L. Mao, H. Qi, D. Xu, H. Huang, M. Liu, Y. Wen, F. Deng, X. Zhang and Y. Wei, *Cellulose*, 2020, **27**, 743–753.
213 H. Xu, S. Huang, J. Wang, Y. Lan, L. Feng, M. Zhu, Y. Xiao, B. Cheng, W. Xue and R. Guo, *Int. J. Biol. Macromol.*, 2019, **137**, 433–441.
214 L. J. Nielsen, S. Eyley, W. Thielemans and J. W. Aylott, *Chem. Commun.*, 2010, **46**, 8929–8931.
215 H. Nawaz, S. Chen, X. Zhang, X. Li, T. You, J. Zhang and F. Xu, *ACS Nano*, 2023, **17**, 3996–4008.
216 J. A. Kelly, A. M. Shukaliak, C. C. Y. Cheung, K. E. Shopsowitz, W. Y. Hamad and M. J. MacLachlan, *Angew. Chem.*, 2013, **125**, 9080–9084.
217 W. Yuan, C. Wang, S. Lei, J. Chen, S. Lei and Z. Li, *Polym. Chem.*, 2018, **9**, 3098–3107.
218 H. Khanjanzadeh and B. D. Park, *Carbohydr. Polym.*, 2021, **273**, 118550.
219 Y. Xiao, Y. Liu, S. Kang, M. Cui and H. Xu, *Food Hydrocolloids*, 2021, **120**, 106893.
220 M. Song, H. Yu, J. Zhu, Z. Ouyang, S. Y. H. Abdalkarim, K. C. Tam and Y. Li, *Chem. Eng. J.*, 2020, **398**, 125547.
221 W. Chen and X. Yan, *J. Mater. Sci. Technol.*, 2020, **43**, 175–188.
222 H. Zhuo, Y. Hu, Z. Chen, X. Peng, L. Liu, Q. Luo, J. Yi, C. Liu and L. Zhong, *J. Mater. Chem. A*, 2019, **7**, 8092–8100.
223 J. Su, L. Zhang, C. Wan, Z. Deng, S. Wei, K. T. Yong and Y. Wu, *Carbohydr. Polym.*, 2022, **296**, 119905.

Open Access Article. Published on 08 Febwaliyo 2024. Downloaded on 12/09/2024 22:53:41.
This article is licensed under a Creative Commons Attribution-NonCommercial 3.0 Unported Licence.

224 J. W. Kim, H. Park, G. Lee, Y. R. Jeong, S. Y. Hong, K. Keum, J. Yoon, M. S. Kim and J. S. Ha, *Adv. Funct. Mater.*, 2019, **29**, 1905968.
225 L. Tang, T. Li, S. Zhuang, Q. Lu, P. Li and B. Huang, *ACS Sustainable Chem. Eng.*, 2016, **4**, 4842–4849.
226 G. Xiao, Y. Wang, H. Zhang, Z. Zhu and S. Fu, *Int. J. Biol. Macromol.*, 2021, **170**, 272–283.
227 Q. Ma and L. Wang, *Sens. Actuators, B*, 2016, **235**, 401–407.
228 C. Sun, D. Zhu, H. Jia, C. Yang, Z. Zheng and X. Wang, *ACS Appl. Mater. Interfaces*, 2020, **12**, 26455–26463.
229 Q. Sun, B. Qian, K. Uto, J. Chen, X. Liu and T. Minari, *Biosens. Bioelectron.*, 2018, **119**, 237–251.
230 A. A. Saeed, M. N. Abbas, B. Singh, R. E. Abou-Zeid and S. Kamel, *Anal. Methods*, 2019, **11**, 6073–6083.
231 Y. Tang, K. Petropoulos, F. Kurth, H. Gao, D. Migliorelli, O. Guenat and S. Generelli, *Biosensors*, 2020, **10**, 125.
232 Q. Liu, Z. Meng, A. Korpi, E. Kontturi and M. A. Kostiainen, *Chem. Eng. J.*, 2021, **420**, 129811.
233 C. T. Tracey, M. A. Torlopov, I. S. Martakov, E. A. Vdovichenko, M. Zhukov, P. V. Krivoshapkin, V. I. Mikhaylov and E. F. Krivoshapkina, *Carbohydr. Polym.*, 2020, **247**, 116704.
234 M. M. Abdi, R. L. Razalli, P. M. Tahir, N. Chaibakhsh, M. Hassani and M. Mir, *Int. J. Biol. Macromol.*, 2019, **126**, 1213–1222.
235 J. V. Edwards, N. Prevost, K. Sethumadhavan, A. Ullah and B. Condon, *Cellulose*, 2013, **20**, 1223–1235.
236 K. Neubauerova, M. C. C. G. Carneiro, L. R. Rodrigues, F. T. C. Moreira and M. G. F. Sales, *Sens. Bio-Sens. Res.*, 2020, **29**, 100368.
237 A. Guyomard-Lack, C. Cerclier, N. Beury, B. Jean, F. Cousin, C. Moreau and B. Cathala, *Eur. Phys. J.-Spec. Top.*, 2012, **213**, 291–294.
238 C. Cerclier, A. Guyomard-Lack, C. Moreau, F. Cousin, N. Beury, E. Bonnin, B. Jean and B. Cathala, *Adv. Mater.*, 2011, **23**, 3791–3795.
239 S. M. Mugo and J. Alberkant, *Anal. Bioanal. Chem.*, 2020, **412**, 1825–1833.
240 W. Ma, L. Xu, L. Wang, C. Xu, H. Kuang, W. Ma, L. Xu, L. Wang, C. Xu and H. Kuang, *Adv. Funct. Mater.*, 2019, **29**, 1805512.
241 H. Altug, S. H. Oh, S. A. Maier and J. Homola, *Nat. Nanotechnol.*, 2022, **17**, 5–16.
242 A. D. Association, *Diabetes Care*, 2010, **33**, S62–S69.
243 K. J. Cash and H. A. Clark, *Trends Mol. Med.*, 2010, **16**, 584–593.
244 L. Dong, X. Zhang, S. Ren, T. Lei, X. Sun, Y. Qi and Q. Wu, *RSC Adv.*, 2016, **6**, 6436–6442.
245 R. Chandrawati, *Exp. Biol. Med.*, 2016, **241**, 972–979.

© 2024 The Author(s). Published by the Royal Society of Chemistry